9-28-2023

Designing peptide amphiphiles as novel antibacterials and antibiotic adjuvants against gram-negative bacteria

Huihua Xing

Vanessa Loya-Perez

Joshua Franzen

Paul Denton

Martin Conda-Sheridan

See next page for additional authors

Authors

Huihua Xing, Vanessa Loya-Perez, Joshua Franzen, Paul Denton, Martin Conda-Sheridan, and Nathalia Rodrigues de Almeida

Journal Pre-proofs

Designing Peptide Amphiphiles as novel antibacterials and antibiotic adjuvants against Gram-negative bacteria

Huihua Xing, Vanessa Loya-Perez, Joshua Franzen, Paul W. Denton, Martin Conda-Sheridan, Nathalia Rodrigues de Almeida

Please cite this article as: H. Xing, V. Loya-Perez, J. Franzen, P.W. Denton, M. Conda-Sheridan, N. Rodrigues de Almeida, Designing Peptide Amphiphiles as novel antibacterials and antibiotic adjuvants against Gram-negative bacteria, *Bioorganic & Medicinal Chemistry* (2023), doi: https://doi.org/10.1016/j.bmc.2023.117481

This is a PDF file of an article that has undergone enhancements after acceptance, such as the addition of a cover page and metadata, and formatting for readability, but it is not yet the definitive version of record. This version will undergo additional copyediting, typesetting and review before it is published in its final form, but we are providing this version to give early visibility of the article. Please note that, during the production process, errors may be discovered which could affect the content, and all legal disclaimers that apply to the journal pertain.

1 **Designing Peptide Amphiphiles as novel antibacterials and antibiotic adjuvants against**
2 **Gram-negative bacteria**

3

4 Huihua Xing[a], Vanessa Loya-Perez[b], Joshua Franzen[c], Paul W. Denton[c], Martin Conda-Sheridan[b],
5 Nathalia Rodrigues de Almeida[b]*

6 [a]Department of Pharmaceutical Sciences. College of Pharmacy. University of Nebraska Medical Center.
7 Omaha, NE, 68198.

8 [b]Department of Chemistry. University of Nebraska Omaha. Omaha, NE, 68182

9 [c]Department of Biology. University of Nebraska Omaha. Omaha, NE, 68182

10 *Current address: Department of Chemistry. Trinity University. San Antonio-TX, 78212.

11 **Graphical abstract**

12 **Highlights**

13 • PA1 (non-active PA) displayed synergistic antibacterial activity against *E. coli* in combination
14   with Vancomycin.
15 • PA2 and PA3 showed broad-spectrum antibacterial activity against both Gram-positive and
16   Gram-negative strains.
17 • PA2 and PA3 were not susceptible to development of bacterial resistance over a period of 21
18   days.
19 • PA1, PA2 and PA3 presented low cytotoxicity against HEK-293 cells.
20 • Preliminary in vivo studies showed over 60% of *G. mellonella* survival after treatment with PA2.

21

22 **Abstract**

23 Gram-negative strains are intrinsically resistant to most antibiotics due to the robust and impermeable
24 characteristic of their outer membrane. Self-assembling cationic peptide amphiphiles (PAs) have the ability
25 to disrupt bacteria membranes, constituting an excellent antibacterial alternative to small molecule drugs
26 that can be used alone or as antibiotic adjuvants to overcome bacteria resistance. PA1 (C_{16}KHKHK), self-
27 assembled into micelles, which exhibited low antibacterial activity against all strains tested, and showed
28 strong synergistic antibacterial activity in combination with Vancomycin with a Fractional Inhibitory
29 Concentration index (FIC*i*) of 0.15 against *E. coli*. The molecules, PA2 (C_{16}KRKR) and PA3
30 (C_{16}AAAKRKR), also self-assembled into micelles, displayed a broad-spectrum antibacterial activity
31 against all strains tested, and low susceptibility to resistance development over 21 days. Finally, PA1, PA
32 2 and PA3 displayed low cytotoxicity against mammalian cells, and PA2 showed a potent antibacterial
33 activity and low toxicity in preliminary *in vivo* models using *G. mellonella*. The results show that PAs are
34 a great platform for the future development of effective antibiotics to slow down the antibiotic resistance
35 and can act as antibiotic adjuvants with synergistic mechanism of action, which can be repurposed for use
36 with existing antibiotics commonly used to treat gram-positive bacteria to treat infections caused by gram-
37 negative bacteria.

38

1. Introduction

Antibiotic resistance still remains one of the greatest health concerns globally, and it has become an even more serious threat following the COVID-19 pandemic. According to a CDC report from 2022[1], the COVID-19 pandemic caused a huge impact in antibiotic resistance due to a lack of data reporting for 9 pathogenic threats and an increased number of antibiotic prescriptions for patients (even though antibiotics are not effective for viruses). Out of the 18 most serious antibiotic-resistant threats listed, 10 are gram-negative strains.[2] For example, the available data show an increase of 78% Carbapenem-resistant *Acinetobacter* infections, 35% of Carbapenem-resistant *Enterobacteriaceae*, 14% of Vancomycin-resistant *Enterococci*, and 13% of Methicillin-resistant *Staphylococcus aureus* compared to the 2019 CDC data.[1] This problem is exacerbated by the fact that many large pharmaceutical companies are no longer investing as much in antibiotic R&D.[3] According to the latest WHO report, only 2 out of 27 antibiotics under development against WHO bacterial priority pathogens meet at least one criteria of innovation or are active against multidrug resistant gram-negative bacteria. To make this situation even more concerning, nearly 80% of the newly approved antibiotics belong to the existing class of antibiotics which bacteria already has developed resistance.[4] Thus, there is an urgent need for alternative strategies to treat bacterial infections.

Gram-negative bacteria are protected from external agents by the presence of the outer membrane (OM) barrier and efflux mechanism. The outer membrane is an asymmetrical lipid bilayer composed of highly packed lipopolysaccharides (LPS) and negatively charged phospholipids which form a robust barrier that is effective at preventing the accumulation of drugs. Antibiotics with activity against gram-negative bacteria are essentially limited to small and hydrophilic drugs with MW lower than 600 Da that can cross the membrane via porins.[5, 6, 7] Moreover, these membrane characteristics make gram-negative bacteria intrinsically resistant to antibiotics[8], limiting the options available to treat these pathogens. In addition to innate resistance, bacteria can also develop resistance against antibiotics via different mechanisms. One of the approaches to overcome this problem includes chemical perturbation or disruption of the outer membrane, allowing the accumulation of antibiotics traditionally active against gram-positive bacteria to permeate inside gram-negative bacteria.[9, 10]

For example, combinations of pentamidine, an antiprotozoal agent used to treat pneumocystis pneumonia, trypanosomiasis, and leishmaniasis, with antibiotics such as minocycline, linezolid, valnemulin, and nadifloxacin have shown enhanced activity against multidrug-resistant bacteria including *Escherichia coli*, *Acinetobacter baumannii*, *Pseudomonas aeruginosa*, *Klebsiella pneumoniae*.[11] Pentamidine also potentialized novobiocin in a dose-dependent manner against colistin-resistant *A. baumannii* in a murine model.[10] However, the toxicity of pentamidine is a big concern. Patients treated with pentamidine often develop nephrotoxicity, hypotension, hypoglycemia, hepatic dysfunction, QT prolongation and leucopenia.[12, 13]

There are also some literature reports showing an increase in efficacy and slow development of resistance when antibiotics are combined with molecules that potentiates their activity.[15-21] For example, cyclic amphiphilic peptides combined with tetracycline, tobramycin, clindamycin, kanamycin, levofloxacin, polymyxin B, metronidazole, and vancomycin have been shown to display synergistic antibacterial activity against *S. aureus, P. aeruginosa, E. coli and K. pneumoniae*.[14] Antimicrobial peptides have been reported to synergize with vancomycin against gram-negative bacteria.[15] Peptidomimetics[16], cell-penetrating peptides[17], small molecule,[18] and synthetic polymers[19,20] also have been reported to enhance the antibacterial activity of existing antibiotics against multidrug-resistant pathogens. These membrane-active compounds are often cationic and/or amphiphilic, and the biggest limitation is their toxicity[12] (ability to disrupt host cell membranes), and poor pharmacokinetics properties including low availability and metabolic stability.[21]

84   Overall, Peptide Amphiphiles (PAs) make an excellent candidate as novel antibiotics and antibiotic
85 adjuvants because they are biocompatible, are less likely to be immunogenic[22] due to use of proteinogenic
86 amino acids, have structural similarities to endogenous peptides, and they are likely to have increased
87 metabolic stability (when compared to linear antimicrobial peptides) due to the presence of an hydrophobic
88 tail and self-assembly into nanostructures.[23,24,25] Still, one of the biggest challenges of antibacterial PAs is
89 the cytotoxicity against mammalian cells and red blood cells. Cytotoxicity toward these cells have been
90 linked to the overall hydrophobicity and the length of the alkyl tail,[26, 27] , but the use of drug combinations
91 is a great approach to overcome the cytotoxicity of these lipopeptides due to significantly lower
92 concentrations needed for antibacterial activity.

93   Aiming to improve specificity of these PAs as antibacterial and antibacterial adjuvants, we
94 designed and synthesized a small library of novel PAs with hexadecanoyl (C_{16}) hydrophobic tails with
95 various basic amino acids (positively charged) residues to target bacteria membranes. According to our
96 previous report, C_{16} tail has showed better selectivity against bacterial strains.[27] We also designed PAs
97 containing octadecanoyl (C_{18}) hydrophobic tails with shorter side chain basic amino acids to decrease the
98 overall hydrophobicity of the PA molecules. We determined the morphology of the self-assembled
99 nanostructures by Transmission Electron Microscopy (TEM). To address whether PAs present antibacterial
100 activity and would synergistically enhance efficacy and availability of antibiotics to reduce bacteria
101 resistance and cytotoxicity, we conducted antibacterial assays to determine Minimum Inhibitory
102 Concentration (MIC), checkerboard assays to study synergy between PAs and antibiotics to determine FIC*i*,
103 Propidium Iodide (PI) uptake to study inner membrane permeability, and bacteria resistance assays to study
104 the antibacterial activity of the assemblies alone and in combination with other antibiotics. We also studied
105 the cytotoxicity of the PAs in HEK-293 and red blood cells and performed a preliminary investigation of
106 *in vivo* antibacterial efficacy using *G. mellonella*.

107

2. Materials and Methods

109 ***2.1. Synthesis of Peptide Amphiphiles (PAs):*** The PAs were synthesized using standard Fmoc Solid Phase
110 Peptide Synthesis (SPPS) according to procedures published in a previous report (Supporting Information
111 (SI1).[28] PAs were prepared either manually or using a Alstra Biotage microwave peptide synthesizer in a
112 0.3 mmol scale using rink amide resin (AAPPTEC). The Fmoc-Rink Amide MBHA Resin was purchased
113 from AAPPTEC (Louisville, KY) and the FMOC L-amino acids and coupling agents including N,N'-
114 Diisopropylcarbodiimide (DIC) and N,N,N′,N′-Tetramethyl-O-(1H-benzotriazol-1-yl)uronium
115 hexafluorophosphate (HBTU) were purchased from AAPPTEC and Novabiochem (MilliporeSigma). Other
116 solvents and reagents including dichloromethane (DCM), dimethylformamide (DMF), N,N-
117 Diisopropylethylamine (DIPEA)and 4-methylpiperidine were purchased from Fisher Chemicals
118 (ThermoFisher Scientific). The chemical structure of the molecules was confirmed by MALDI-TOF-MS
119 (SmartFlex bench top MALDI-TOF MS Bruker and Bruker's Autoflex maX MALDI-TOF/TOF). The
120 products were purified using a preparative reverse phase high-performance liquid chromatography (RP-
121 HPLC; Agilent) in a C18 column as the stationary phase of 5 μm, 100 Å pore size, and 150 × 21.1 mm
122 (Phenomenex) with a gradient of ACN/H_2O (containing 0.1% of trifluoroacetic acid - TFA). The purity of
123 the new PAs was confirmed by an analytical HPLC instrument using a C18 column at a wavelength of 220
124 nm with a linear gradient of ACN/H_2O (0.1% TFA) from 5 to 95% for 30 min. The pH of the water solution
125 was adjusted to 7 and then lyophilized using a Labconco FreeZone Benchtop Freeze Dryer. All PA samples
126 were self-assembled in ultrapure water at 1 mg/mL and the pH was adjusted to 7. The solutions were heated
127 to 70˚C for 2 h and incubated at r.t. overnight before testing.

128

129   **2.2. Zeta Potential:** The PA samples were prepared at 1mg/mL concentration, the pH was adjusted to 7 by
130   addition of HCl or NaOH), annealed at 80 °C for 2 hours, and aged overnight. Before the experiment, the
131   PA solutions were diluted to 250 µg/mL in HPLC grade water. Zeta Potential was determined using a
132   Zetasizer NanoZS (Malvern Instruments) at 25 °C. For bacteria assays, *S. aureus* JE2 and *E. coli* K12 were
133   cultured in Muller−Hinton broth (MHB) to mid logarithmic-phase (OD. ~ 0.8). . Bacteria cells were washed
134   and resuspended in PBS to 5×10^7 colony forming unit per mL (CFU/mL) and treated with PAs at 10 ×
135   MIC for 1 h before the zeta potential measurements. Polymyxin B and Daptomycin were used as standard
136   drugs and bacteria cells without treatment were used as negative control.

137   **2.3. Transmission Electron Microscopy (TEM):** The PAs were dissolved in HPLC grade water to give a
138   final concentration of 2 mM and pH was adjusted to 7, which is near physiological pH. Our previous study
139   have shown that salt concentration (lower than 1M concentration) has a minimal effect on the morphology
140   of similar structures in this manuscript (i.e, $C_{16}K_2$ and $C_{16}K_3$).[29] In addition, we have reported that self-
141   assembly in different conditions (e.g. changing counter ion) has no effect on the antimicrobial activity of
142   PAs.[27] The samples were incubated at room temperature overnight before the experiments. Approximately,
143   6µL of the sample was applied onto a copper grid and allowed to absorb for 5 min, covered with a folded
144   piece of filter paper like a tent. The excess PA was removed from the grid by inverting the forceps and
145   touching only the edge of the grid to a clean piece of the filter paper. Then, 6µL of the negative stain
146   (NanoVan) was added for 30 seconds. The excess stain was removed, and the PAs were imaged with a FEI
147   TEcnai G2 Spirit transmission electron microscope (120 kV), and an AMT digital imaging system.
148
149   **2.4. Minimal Inhibitory Concentration (MIC):** The MICs were determined using the broth microdilution
150   method as previously described.[27] Bacterial cultures were made by the direct colony suspension method to
151   1.5×10^8 colony forming unit per mL (CFU/mL) (0.5 McFarland) and diluted in Muller−Hinton broth
152   (MHB) to a final concentration of $\sim10^5$ CFU/mL. A stock solution of each PA to be tested was prepared in
153   HPLC grade water at 1mg/mL concentration and pH was adjusted to 7. The dilutions were made in MHB
154   (100 µL per well), in 96-well plates (Greiner, Bio-One), after that, each well was inoculated with 10 µL of
155   bacterial cultures and plates were incubated for about 20-24 h at 37 °C. The lowest concentration of PA
156   that inhibits bacterial growth was considered the MIC. The optical density (O.D.) was recorded using an
157   AccuSkan, MultiSkan FC (Thermo Fisher Scientific) at 600 nm. Vancomycin and Gentamicin were used
158   as positive controls and media was used as negative control. Samples were tested in triplicate. 1% 2,3,5-
159   Triphenyltetrazolium chloride (TTC) solution was used to stain for easier visualization.

160   **2.5. Checkerboard Assay:** *E. coli* K12 and *A. baumannii* clinical strain (deidentified strain collected in the
161   clinical microbiology laboratory at Nebraska Medicine) were grown overnight to mid logarithmic phase
162   (OD. ~ 0.8) in MHB medium and diluted in MHB to $\sim10^5$ CFU/mL. Antibiotic synergy was determined
163   using checkerboard broth microdilution assays with two-fold serial dilutions of antibiotics (Rifampicin and
164   Vancomycin) across the 96-well plate (Greiner, Bio-One), (horizontal) and two-fold serial dilutions of PAs
165   down the plates (vertical) to final volumes of 100 µL. After the serial dilutions were made, 10 µL of bacteria
166   culture were added to each well and the plates were incubated for 20-24h at 37 °C. The O.D. was recorded
167   with an AccuSkan, MultiSkan FC (Thermo Fisher Scientific) at 470 nm. Fractional inhibitory concentration
168   index (FICi) was calculated according to the following equation (equation 1):

169

170
$$FICi = \frac{MICac}{MICa} + \frac{MICbc}{MICb} = FICa + FICb$$

171 where *MICa* is the MIC of compound A alone; *MICac* is the MIC of compound A in combination with
172 compound B; *MICb* is the MIC of compound B alone; *MICbc* is the MIC of compound B in combination
173 with compound A; *FICa* is the FIC of compound A; *FICb* is the FIC of compound B. Synergy as defined
174 as an *FICi* of ≤0.5[11], Additive and indifference was defined as an FICi of 0.5–4[11] and Antagonism was
175 defined as an *FICi* of ≥4.[11]

176 **2.6. Bacteria Resistance Studies:** The resistance induction studies were performed in *S. aureus* JE2 and *E.*
177 *coli* K12 using broth microdilution method after 21 passages following procedures described in the
178 literature.[30,31] and the MIC values were assessed after every passage. 21 days is an appropriate time frame
179 because of the fast cell division of bacteria. For example, others have investigated the development of
180 bacteria resistance against antibacterial nanoparticles over periods of 5-15 days.[32] On day 1, the MIC value
181 for the PAs was assessed using the MIC assay method described above. On day 2-21, the MIC assays for
182 PAs and vancomycin were performed with at least 3 concentrations above and 3 concentrations below
183 previous MIC values (1/8 MIC, 1/4 MIC, ½ MIC, MIC, 2xMIC, 4xMIC, and 8xMIC). The bacteria
184 suspension at the sub-MIC concentration from the previous day was diluted to 1.5×10^8 colony forming
185 unit per mL (CFU/mL) (0.5 McFarland) in MHB. The bacteria culture was further diluted in MHB to a
186 final concentration of 1.5×10^5 CFU/mL and 100 μL was added into the serial-diluted assay plate
187 containing the PAs. The plate was incubated at 37 ℃ for 20-24 h, and 1% TTC solution was used to stain
188 for easier visualization. The MIC tests were repeated for 21 days.

189 **2.7. Propidium iodide (PI) uptake:** *E. coli* K12 cells were grown in MHB to the mid logarithmic-phase and
190 the bacterial cells were separated by centrifugation at 5000 rpm for 15 min and washed twice with HyClone
191 Dulbecco's phosphate buffered saline (PBS) solution (GE Healthcare Life Science). Bateria cells were
192 diluted to 10^6 CFU/mL using 5 mM HEPES buffer + glucose. Bacteria suspensions containing 2 mM of PI
193 were incubated at 37 °C for at least 15 mins before treatment withPAs and antibiotics. . In a 96-well plate,
194 40 μL of PAs andVancomycin at different concentrations (1/8 MIC, 1 × MIC, and 2 × MIC) and the PA-
195 Vancomycin drug combination (1:1 ratio of PA-Vancomycin) were added to each well. Then, 160 μL of
196 PI-stained bacteria solution was added to each well. Polymyxin B was used as a reference drug (positive
197 control) and cells with no antibiotic treatment were used as a negative control. The PI fluorescence was
198 measured using a spectrofluorometer (SoftMax Pro7.1 and SpectraMax M5[e]) with excitation and emission
199 wavelengths set at 535 nm and 615 nm, respectively.

200 **2.8. Scanning Electron Microscopy (SEM):** *S. aureus* JE2 and *E. coli* K12 were grown in MHB at 37 °C
201 and the resultant mid-log phase culture was diluted in PBS (GE Healthcare Life Science) to a final
202 concentration of 1.5×10^8 CFU/mL. The bacteria cells were treated with PA2 at twice the MIC value and
203 then incubated for 2 hours at 37 °C. Untreated cells (with no PA added) were used as a control. After the
204 incubation, the bacteria cells were washed three times with PBS and the samples were fixed in a solution
205 of 2.0% (v/v) glutaraldehyde and 2% (v/v) of paraformaldehyde in phosphate buffer (0.1 M, pH 6.2) for 24
206 hours at 4 °C. The samples were placed on glass chips coated with 0.1% poly-L lysine, allowed to adhere
207 for 30 min and then washed three times with PBS. After fixing, samples were treated with a 1% aqueous
208 solution of osmium tetroxide for 30 min to aid in conductivity. After that, samples were dehydrated in a
209 graded ethanol series (50, 70, 90, 95 and 100% EtOH solutions). Then, samples were critical point dried
210 and attached to aluminum SEM stubs with double-sided carbon tape. Silver paste was applied to increase
211 conductivity. The following day, samples were coated with ∼50 nm gold–palladium alloy in a Hummer VI
212 Sputter Coater (Anatech USA) and imaged at 30 kV in a FEI Quanta 200 SEM operating in high vacuum
213 mode.
214
215 **2.9. Cytotoxicity:** HEK-293 cells were cultured using ATCC protocols at 37°C in a humidified environment
216 with 5% CO_2 and passages 3-8 were used for all the experiments. The assays were carried out in sterile 96-

217   well flat-bottomed polystyrene microtiter plates (Greiner, Bio-One). Plates containing 100 μL of cell
218   suspension (5×10^4 per well) in each well were preincubated for 24 h at 37 °C in a humidified environment
219   with 5% CO_2. In the following day, the PA samples were serial diluted in a new 96 well plate. The old
220   media was then replaced by the PA solutions and incubated for 24 h. Samples were run on each plate in
221   triplicate and the final concentrations of PAs ranged from 8 to 256 μg/mL. The plates were further incubated
222   with 50 μL XTT reagent (0.5 mg/mL) at 37 °C for 4h. The absorbance of the solution was determined at
223   600 nm using a multiwell plate reader AccuSkan, MultiSkan FC (Thermo Fisher Scientific).
224

225   ***2.10. Hemolysis Assay:*** The cytotoxicity against human red blood cells was adapted as described by Nielson
226   et al 2021. Fresh human red blood cells (hRBCs) were washed three times with PBS buffer, centrifuged at
227   500 x g for 5 min, decanted, and then resuspended in PBS to a concentration of 0.5×10^8 cells/mL. PA
228   stock solutions were prepared in ultrapure water at concentrations ranging from 16 to 1024 μg/mL and 25
229   μL were added to a 384-well plate. Then, 25 uL of cell suspension in PBS was added to each well to a final
230   concentration of 0.25×10^8 cell/mL. The plate was then shaken for 10 minutes on a microplate shaker before
231   incubation at 37°C in 5% CO_2 for 60 min, and the cells were pelleted by centrifugation at 1000 x g for 10
232   minutes. Lastly, 25 μL of the supernatants were transferred to a new 384-well plate, flat-bottomed plastic
233   384-well plate and the concentration of hemoglobin was determined by measuring the OD at 405 nm using
234   a BioTek Synergy LX plate reader. The absorbance of the supernatants of cells incubated with 5% Triton
235   X-100 (positive control) were considered 100% hemolysis, ultrapure water was used as a negative control.
236

237   ***2.11. pH-Dependent Cytotoxicity Assay:*** HT-29 cells (ATCC HTB-38) were cultured in McCoy's 5a
238   Medium Modified (ATCC 30-2007) with 10% fetal bovine serum and 1% penicillin/streptomycin. 100 μL
239   of HT-29 cell suspension was added to each well of sterile, polystyrene 96-well plates (Nunclon - Delta
240   Surface treated) at a concentration of 150,000 cells/mL (15,000 cells/well) and incubated at 37°C in 10%
241   CO_2 for 24 hours. Following the 24-hour incubation, the culture media was removed and replaced with
242   either 100 μL of fresh media (pH 7.4) or acidified media (pH 6.5). The acidified media was prepared by
243   adding MOPS (3-(N-morpholino)-propanesulfonic acid; Alfa Aesar J62840; CAS 1132-61-2) to reach a
244   concentration of 20 mM, and then lowering the pH to 6.5 using HCl. Stock solutions of the treatment
245   peptides were prepared at 5 mg/mL in deionized water. From the stock solution, treatment concentrations
246   were prepared using 2-fold dilutions with the respective treatment media (pH 7.4 or pH 6.5), ranging from
247   7.8 μg/mL -500 μg/mL. Water was used as a negative control and Triton-X 100 (Fisher Bioreagents BP151-
248   500; CAS 9002-93-1) was used as a positive control. Cells were incubated at 37°C in 10% CO_2 for 24
249   hours. Following this incubation period, the media was removed from the wells, each well was washed with
250   100 μL of PBS (phosphate buffered saline; Corning 21-040-CV), and then fresh media (pH 7.4) was added
251   to the wells. The cytotoxicity was measured using an MTT assay kit. 10 μL of 12 mM MTT solution was
252   added to each well, and then cells were incubated at 37°C in 5% CO_2 for 4 hours. 100 μL of SDS-HCl was
253   then added and mixed before incubating again at 37°C in 5% CO_2 for 4 hours. Wells were then mixed, and
254   absorbance was read at 570 nm using a BioTek Synergy LX plate reader.
255

256   ***2.12. In vivo Antibacterial Studies:*** *Galleria mellonella* were purchased from Bestbait (Lakeside
257   Marblehead, OH, USA) and maintained on wood chips in the dark. And all assays were followed by the
258   published protocol.[33] Five to nine larvae with a mass of ~160-190 mg each, without darkening of the cuticle,
259   were selected for each step in the procedure. The bacteria suspension was injected into the last left proleg
260   (Hamilton neurons syringe 25 μL, 33-gauge, point style 4, angle 12˚). The larvae were incubated at 37˚C
261   for 2-4 days and mortality was recorded daily. **Determination of bacterial infection**: To determine the
262   bacterial infection, 10 μL of various concentrations of MRSA JE2 (1.5×10^7 cfu and 1.5×10^8 cfu) were
263   injected and incubated for 2 days at 37 ˚C to mimic infection in humans. An infective dose of bacteria was

264 determined to cause 60-80% lethality within 48 h, but not 100% lethality within 24 h. ***In vivo* Toxicity**
265 **testing procedure:** Based on the OECD guidelines, the acute toxicity testing was started by injecting five
266 larvae with the initial dose of a 25 mg/kg. The toxicity testing was continued by retesting at the same dose
267 on new cohort of larvae, if less than 40% lethality was achieved. The experiment continued until a toxic
268 dose was established. ***In vivo* Antibacterial efficacy assay:** First, 10 µL of bacteria at the pre-determined
269 infective dose were injected into the last left proleg and incubated for 2h. After incubating, 10 µL of PA
270 compound or antibiotic was injected to the last right proleg and returned to incubation at 37 ˚C. The
271 mortality was recorded daily for 4 days. Vancomycin was used as a positive control. Infected animals
272 without treatment were used as negative control and animals injected with PBS only were also used as a
273 control.

274 ## 3. Results and Discussion

275 ### 3.1. Design and characterization of the PAs

276 According to our previous report[27], the antimicrobial activity and cytotoxicity of PAs are strongly
277 correlated to the length of their hydrocarbon chain. PAs containing an 18-carbon long hydrophobic tail
278 displayed greater antimicrobial activity but also high cytotoxicity against human cells (including HEK-293
279 and red blood cells) than the counterparts with shorter alkyl tails. The 16-carbon length PAs showed a
280 diminished antibacterial activity but lower toxicity against human cells compared to their 18-carbon
281 counterparts. Aiming to develop more selective PAs and further study the effects of the 16-carbon length
282 hydrophobic tail in the antibacterial activity of these peptides, we designed cationic PAs with a 16-carbon
283 hydrophobic tail while varying their amino acid sequence. In particular, we studied Lysine (Lys), Arginine
284 (Arg), Histidine (His), and Tryptophan (Trp). Lys, Arg are known as important cationic amino acids that
285 interact with negatively charged lipids present in bacteria membranes[34] and replacement of Lys with His
286 residues have shown decreased cytotoxicity while maintaining antibacterial activity.[35] Trp residues are
287 known to facilitate bacteria membrane disruption and improve the activity of antimicrobial peptides due to
288 its hydrophobic characteristics. Trp interacts with the interface region in the membrane, helping the peptide
289 to anchor to the bilayer surface.[36] We also designed PAs containing a 18-carbon length tail to
290 diaminopropionic acid (Dap). Dap is a non-proteinogenic amino acid, with shorter side chain (1 methylene
291 unit, less hydrophobic) than Lys. This amino acid has a $pK_a \sim 6.0$ which will be deprotonated at
292 physiological pH. However, there is most likely a small variation since the pKa values for amino acids can
293 vary depending on the chemical environment and proximity to the core of the nanostructure, similar to the
294 shifts of pKa that happens in folded proteins.[37, 38] The structure of the designed PAs, the morphology of the
295 self-assembled structures they form, and their physical chemical properties are summarized in Table 1.

296 **Table 1: Sequence, morphology, and physicochemical properties of PAs**

PAs	Sequence[a]	Morphology by TEM	Charge at pH 7[b]	Charge at pH 5.5[b]	Zeta Potential (mV)[c]	Retention Time (min)[d]
PA1	$C_{16}KHKHK$	Spherical micelles	+3	+5	15.8 ± 1.9	13.4
PA2	$C_{16}KRKR$	Spherical micelles	+4	+4	15.0 ± 8.8	13.8
PA3	$C_{16}AAAKRKR$	Spherical micelles	+4	+4	10.8 ± 6.4	14.3
PA4	$C_{16}KKKWW$	Amorphous	+3	+3	47.0 ± 2.0	15.2
PA5	$C_{16}FFFKKKK$	Nanofibers	+4	+4	11.9 ± 3.9	16.2
PA6	$C_{18}Dap_5$	Spherical micelles	0	+5	13.7 ± 2.4	14.6
PA7	$C_{18}AADap_3$	Spherical micelles	0	+3	10.3 ± 3.2	15.9
PA8	$C_{18}HHDap_3$	Spherical micelles	0	+5	30.4 ± 3.6	14.4
PA9	$C_{18}RRDap_3$	Spherical micelles	+2	+5	30.1 ± 4.4	14.6

297 [a]Lysine (K, Lys), arginine (R, Arg), phenylalanine (F, Phe), alanine (A, Ala), histidine (H, His), tryptophan
298 (W, Trp), Dap (DAP (2,3-diaminopropionic acid), hexadecanoic acid (C16) and octadecanoic acid (C18).

299 ⟨b⟩Estimated charges based on pK_a values for individual amino acids. ⟨c⟩Aqueous solution of 250 µg/mL
300 concentration at pH 7. ⟨d⟩Retention time obtained from RP-HPLC analysis using a linear gradient method of
301 ACN:$H_2$0 containing 0.1% TFA (0-100% 20 mins).

302

303 The chemical structures, mass spectra and purity of the compounds can be found in the Supporting
304 Information (SI1). The morphology of the self-assembly nanostructures was assessed by transmission
305 electron microscopy (TEM) and shown in Figure 1 and Figure SI5. As expected, PA1, PA2, PA3, and PA6,
306 PA7, PA8 and PA9 self-assembled into micelles, a morphology driven by the hydrophobic collapse of the
307 tails and the repulsion between the charged residues.[39] PA2 formed micelles with 7 +/-1 nm width. The size
308 of the other nanostructures could not be determined because they were too small for accurate measurement
309 with our instruments. . Interestingly, we expected that PA3 would self-assemble into fibers due to Ala
310 residues adjacent to the hydrophobic tail that have propensity to for β -sheets. A possible factor that leads
311 to the formation of micelles instead of nanofibers could be related with the ionic strength and strength of
312 the intramolecular bonding[39] since both hydrophobic interactions and hydrogen bonding are present in the
313 same molecule, the decreased ionic strength increase the electrostatic repulsion of the charged residues[40]
314 favoring the formation of micelles. PA3 only contains 3 Ala residues, which is not enough to produce
315 sufficient H-bonds to offset the electrostatic repulsion. According to previous report, the formation of fibers
316 is favored by 4 amino acid residues forming β-sheet hydrogen bonds close to the core.[41] This could also be
317 observed in PA7, which contain 2 Ala residues and self-assemble into micelles (Table 1). PA4 did not self-
318 assemble into nanostructures possibly due to the bulky Trp residues being placed in the C-terminus of the
319 peptide structure. The lack of backbone H-bonding and the electrostatic repulsions near the hydrophobic
320 portion could be other factors influencing the formation of well-defined nanostructures. PA5 self-assembled
321 into nanofibers with ~ 9 nm of diameter, due to the π-π stacking of the phenylalanine residues, which also
322 works as a promoter for both α-helix and β-sheet. Thus, a better ability for fibril formation is achieved when
323 compared to PA5. TEM images for selected PAs are shown in Figure 1, while the rest of the other TEM
324 images can be found in the supporting information (SI 5).

325
326
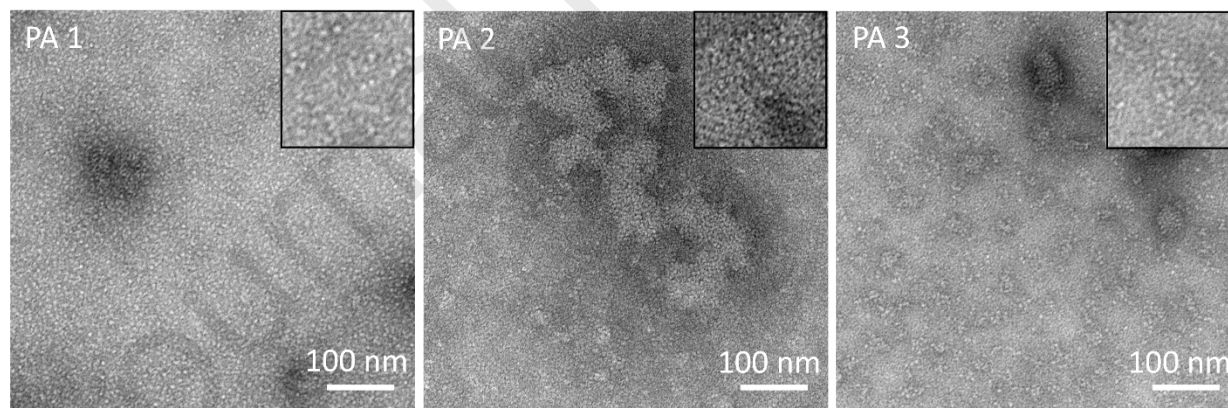
Figure 1. Morphology of PA 1, PA 2, and PA 3 assemblies observed by TEM. PA was prepared at 1 mg/mL in HPLC grade water, annealed, and aged overnight before imaging. Scale bar 100 nm. All these three PAs formed 6-7 nm diameter spherical micelles.

327
328
329

330 Charge and hydrophobicity have been described to be important for antimicrobial activity of
331 peptides. The positive charge facilitates the interaction with the slightly negative bacteria membrane and
332 the hydrophobic alkyl chain permeates it, potentially leading to membrane damage. We studied the zeta
333 potential to determine surface charge and hydrophobicity of the PAs and the values are shown in Table 1.
334 All peptides showed positive zeta potential values ranging from +10.3 to +47 mV. PA3, PA5, PA6 and PA7

335   are considered nearly neutral with zeta potential values around + 10 mV. PA6 and PA7 are composed by
336   Dap as a cationic residue which is not expected to be protonated at pH 7, which is consistent with the lower
337   zeta potential values. The relatively smaller zeta potential values of PA2, PA3, and PA5 indicate a weaker
338   electrostatic repulsion between individual PA molecules that can be related to their morphology. PA2 and
339   PA3 self-assembled into small spherical micelles and some aggregation can be observed from TEM,
340   indicating the tendency for particles to come together. Meanwhile, the entangled PA5-fibers suggest fiber-
341   fiber attraction, probably due to the compromise repulsion due to intermolecular π-π interactions and H-
342   bondings.[42] High repulsive forces between adjacent PA fibers could discourage any lateral
343   assembly/entangle/aggregation.[43] PA4, PA8 and PA9 had large positive zeta potential values being
344   considered strongly cationic. The zeta potential results for PA4 could be explained by the fact this peptide
345   is not self-assemble into nanostructures having all the positive charged residues exposed to the solvent. We
346   also determine the relative hydrophobicity of the PAs using RP-HPLC, retention times are listed in Table
347   1. As expected, PAs with a C18 alkyl chain were among the most hydrophobic PAs showing higher
348   retention time in between 14.44 and 16.19 minutes. PA4 and PA5 have a C16 alkyl chain but displayed a
349   higher hydrophobicity due to the presence of Phe and Trp residues.

350

3.2 PAs shown potent broad-spectrum antibacterial activity against all the strains tested

352   The antibacterial activity of the PAs against gram-negative and gram-positive strains was
353   determined using the broth microdilution method. MIC values are summarized in Table 2. PA2 and PA3
354   displayed potent antibacterial against all tested strains with a geometric mean of MIC values of 6 µg/mL
355   and 7 µg/mL respectively (MICs ranging from 4-8 µg/mL). These PAs are formed by cationic amino acids,
356   Lys and Arg residues are known to have an important role in the activity of Antimicrobial Peptides (AMPs),
357   and they can form hydrogen bonds, electrostatic interactions, and cation-π interaction facilitating the
358   interaction with negatively charged lipids such as lipopolysaccharides and phospholipids in the bacteria
359   membrane.[44]

360   The order of increased zeta potential is as follows: PA7 < **PA3** < PA5 < PA6 < **PA2** < PA1 < PA9
361   < PA8 < PA4 (Table 1). The most active peptides, PA2 and PA3 (in bold) have small Zeta Potential values
362   of 15.0 mV and 10.0 mV, respectively (Table 1). PA1 has a slightly greater Zeta Potential compared to PA2
363   and also a lower antibacterial activity, suggesting that there is a smaller range of values that correspond to
364   biological activity. Another important characteristic of these active peptides is their self-assembling
365   morphology. PA2 and PA3 self-assembled into micelles, and these results support our previous findings
366   that the antibacterial activity is also dependent of the morphology of the nanostructures with micelles
367   demonstrating more potent antibacterial activity compared to nanofibers.[27] Our proposed mechanism of
368   action is that micelles disassemble in contact with bacteria membrane and the hydrophobic moiety of single
369   molecules interact with bacteria membrane and penetrating the lipid bilayer leading to membrane damage.
370   Thus the stability of the nanostructure also plays an important role since micelles in general are less stable
371   compared to nanofibers.[27] The zeta potential experiments are an important tool to determine not only the
372   nanostructure surface charge and propensity to form aggregates but also the stability of the nanoparticles.[45]
373   The smaller zeta potential (generally smaller than +/- 30 mV) values of these peptides indicate low physical
374   stability of the nanostructures which can be related with their potent antimicrobial activity. A recent study
375   investigated the relationship between physical properties and antimicrobial activity of PAs, their findings
376   indicate that less stable nanofibers disassemble in solution resulting in higher antibacterial activity in
377   contrast to more stable nanofibers, which can attach to the bacteria membrane but do not have the ability
378   permeate the membrane leading to lower antibacterial activity. [46] Together, these findings further support
379   our proposed mechanism of action of PA micelles.

The order of increasing relative hydrophobicity of the designed PAs determined by RP-HPLC is as follows: **PA1** < **PA2** < **PA3** < PA8 < PA9 < PA6 < PA4 < PA7 < PA5 (Table 1). The most active PAs, PA2 and PA3 were among the less hydrophobic PAs with retention times of 13.8 and 14.3 min, respectively. This data also suggests that there is a hydrophobicity range ideal for antibacterial activity. It is worth mentioning that PA5 and PA6 are within the zeta potential range for antibacterial activity between ~10-15 mV, but they were more hydrophobic than PA2 and PA3, thus falling outside of the hydrophobicity range (~ 13-14 min) for the antimicrobial activity. This high hydrophobicity might be linked to their lower antibacterial activity.

Table 2: Minimum Inhibitory Concentration (MIC) of PAs against selected bacteria strains

PAs	Sequence	MIC (μg/mL)					
		Ec^a	Ab^b	Sa^c	Sa^d	Sa^e	G.M.
PA1	C_{16}KHKHK	32	64	64	32	n.e.	45.
PA2	C_{16}KRKR	4	8	4	8	8	6.
PA3	C_{16}AAAKRKR	8	4	8	8	8	7.
PA4	C_{16}KKKWW	128	64	128	32	n.e.	76.
PA5	C_{16}FFFKKKK	64	64	64	64	n.e.	64.
PA6	C_{18}Dap$_5$	32	64	32	16	n.e.	32.
PA7	C_{18}AADap$_3$	32	64	32	64	n.e.	45.
PA8	C_{18}HHDap$_3$	64	64	64	32	n.e.	54.
PA9	C_{18}RRDap$_3$	32	32	32	16	n.e.	27.
Vancomycin		n.e.	n.e.	0.5	1	2	
Gentamicin		1	1	n.e.	n.e.	n.e.	

n.e.= not evaluated [a]*Escherichia coli* K12, [b]*Acinetobacter baumannii* (patient isolated from Nebraska Medicine), [c]*Staphylococcus aureus* JE2 MRSA, [d]*Staphylococcus aureus* 13C MRSA, [e]*Staphylococcus aureus* LAC MRSA. G.M.=geometric mean.

The PAs containing His and Dap in their sequence, PA1 and PA6-PA9, demonstrated moderate to lower antibacterial activity with higher MIC values ranging from 16 to 128 μg/ml. His (pK_a~6.3[47]-6.5[48] and Dap (pK_a~6.3[49]) has a neutral side chain at pH 7 with overall charge of these peptides ranging range from 0 to +3, which could explain their lower antibacterial activity. The antimicrobial activity of His rich peptides is reported to be enhanced by acidic pH environments.[50,48] The pH sensitive peptides can be extremely beneficial clinically because it potentially restricts the antibacterial activity to certain compartments of the cellular environment (i.e., acidified phagosome) or certain tissues and organs. This approach can potentially increase selectivity of the peptides since the excessive net charge is reported to cause cytotoxicity,[51] Leveraging pH sensitive peptides is a great opportunity to develop future pH-dependent drug delivery systems with synergistic mechanism of action. Moreover, the replacement of Lys and Arg with Dap in the polar face of AMPs is reported to eliminate lysis of human red blood cells while maintaining the antibacterial activity.[52] We evaluated the antimicrobial activity of PA1, PA2, PA7-PA10 at pH 5.5 against *S. aureus JE2* and *E.coli* K12, however the difference in MIC values were generally small- either equal or 1 fold-increase in activity compared to the MIC at pH 7.0 (Supporting Information SI6), and these small differences likely have minimal physiological relevance. We were expecting a better antimicrobial activity, especially for PA7 and PA9, which are completely neutral at pH 7 and have a +5 charge at pH 5.5. However, we now believe that the short side chain of Dap (1-carbon length) is less available to bind and interact with negative charge lipids in the membrane, thus not leading to an increased antibacterial activity. This is also known as "snorkel effect", which explains that longer aliphatic side chain (i.e. lysine and arginine) of the positive charged residues are able to insert deeply into the lipid membrane while still interacting with

412 negatively charged lipid membrane on the surface[53, 54]. Together, our findings and data in the relevant
413 literature explain the relatively poor antibacterial activity of PA7, PA8, PA9 and PA10.

414 Tryptophan has been reported to enhance antibacterial activity of peptides due to its hydrophobic and bulky
415 side chain that facilitates the binding of the peptide to the lipid bilayer via interactions with the interfacial
416 area of the cell membrane, therefore we would expect that PA5 would present antibacterial activity[55]. The
417 positively charged Lys residues in the PA5 are (most likely) less available to interact with LPS in the
418 bacterial membrane because they are placed between the long hydrocarbon chain and two bulky tryptophan
419 residues, making it more difficult to target the membrane via electrostatic interactions. In addition, PA5
420 does not self-assemble into a well-defined nanostructure. Together, our findings suggest that the
421 antibacterial activity is not only related to the proper balance of charge and hydrophobicity, the amino acid
422 composition, the morphology of self-assemble and the stability of these nanostructures most likely also
423 play an important role in their interaction with bacterial membrane.

424 Lastly, we tested the ability of PA2 to inhibit the formation of biofilms and disrupt biofilm. PA2 was not
425 able to disrupt pre-formed S. aureus JE 2 biofilms at the MIC, 2 times MIC and 4 times MIC concentrations,
426 however PA2 was able to inhibit the formation S. aureus JE 2 biofilm at MIC concentration (Methods and
427 results are described in the Supporting Information SI7).

3.3. PA1 potentiates the activity of vancomycin against E. coli leading to a synergistic antibacterial activity

430 We tested some selected PAs based on their antibacterial activity, in combination with Rifampicin and
431 Vancomycin to evaluate synergistic antibacterial activity using a checkerboard assay. Drug combinations
432 with FICi below 0.5 indicates a synergistic antibacterial effect and FICi between 0.5 to 4 indicates an
433 additive or indifferent effect[11]. To be considered a good antibiotic adjuvant candidate, it should exhibit a
434 synergistic effect with antibiotics with FICi below 0.5 associated with a low antibacterial activity (higher
435 MIC value) of the antibiotic alone.

436 Rifampicin is a lipophilic drug and a potent antibiotic that inhibits the synthesis of RNA by binding
437 the DNA-dependent RNA polymerase[56], and it is not typically used against gram-negative bacteria due to
438 limitations in the membrane permeability. Figure 2 shows the checkerboards of PA2 and PA3 in
439 combination with Rifampicin against *E. coli* and *A. baumannii*. PA2 and PA3 alone displayed antimicrobial
440 activity against *E. coli* and *A. baumannii,* as described previously, with MICs ranging from 4-8 µg/mL
441 (Table 2). Thus, if rifampicin shows increased antibiotic activity against gram-negative bacteria in
442 combination with PAs, then it would likely suggest synergistic or additive activity due to PA-induced
443 membrane permeability. Rifampicin (MIC=8µg/mL against *A. baumannii* and *E.coli*) presented a 2-fold
444 increase in antibacterial activity against *A. baumannii* in combination with PA2 and PA3 with FICi of 0.75,
445 whereas rifampicin displayed an 8-fold increase in antibacterial activity against *E. coli* when in combination
446 with PA3 and PA4 with FIC of 0.67, indicating an additive effect or "no interaction" between these drugs.[57]
447 In general, the outer membrane permeabilizer compounds that potentiate the activity of gram-positive
448 antibiotics in gram-negative strains present very low or no antibacterial activity alone[58], a well-known
449 example is the Polymyxin B nonapeptide (PMBN) which possess a very low antibacterial activity alone but
450 is able to potentiate the antibacterial activity of several antibiotics against gram-negative bacteria including
451 Rifampicin.[59] Thus, the "no interaction" between PA2 and PA3 with rifampicin could be explained by the
452 fact that these PAs already present antibacterial activity alone.

453 Gram-negative bacteria are intrinsically resistant to vancomycin blocking its access to lipid II target.[9] We
454 evaluated the effect of PA1, a compound with low antibacterial activity (MIC= 32 µg/mL against *E.coli*)
455 in combination with vancomycin against *E. coli* (Figure 2). The findings of this combination were very

456 interesting as vancomycin exhibited a 32-fold increase in antibacterial activity with the presence of PA1
457 (MIC_{Vanco}= 128 µg/mL and $MIC_{Vanco+PA1}$=4 µg/mL). Thus, PA1 can work as a membrane-targeting
458 compound to potentiate the activity of vancomycin. In addition, the activity of PA1 itself is also enhanced
459 by the presence of vancomycin asPA1 exhibits an 8-fold increase in antibacterial activity (MIC_{PA1}= 32
460 µg/mL and $MIC_{PA1+Vanco}$=4 µg/mL), leading to a synergistic antibacterial activity with FICi of 0.15.

461
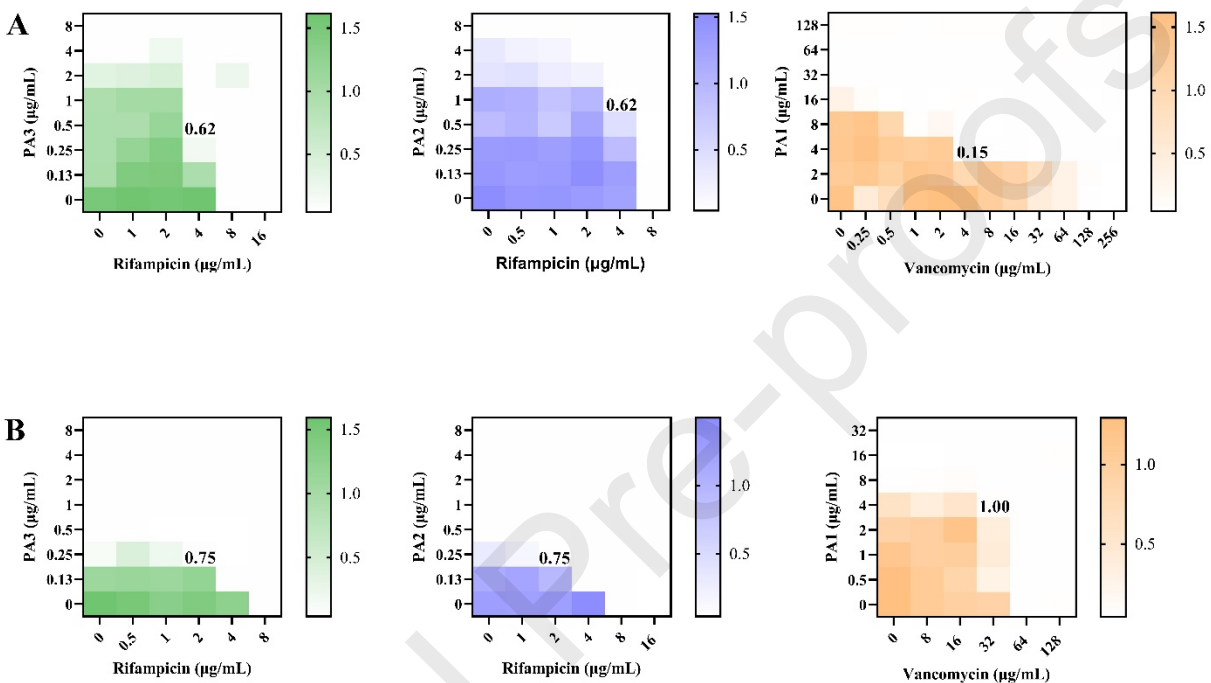
Figure 2: Synergistic screening of selected PAs in combination with antibiotics. A) Checkerboards of PA3 and PA2 in combination with Rifampicin and PA1 in combination with Vancomycin against *E. coli.* B) Checkerboards of PA3 and PA2 in combination with Rifampicin and PA1 in combination with Vancomycin against *A. baumannii.* FICi`s are shown in the figure. Selected antibiotics were tested at 2-fold serial dilutions across the plate in combination with 2-fold serial dilutions of the selected PAs down the plate, where the last column and the last row in the plate contain two-fold dilutions of antibiotics and peptides alone to determine their MIC.

462

463

464 In addition, we tested the PA1 and PA5 in combination with vancomycin against *A.baumannii*. We
465 observed no significant effect of these combinations which can be explained by the more permeable OM
466 of *E. coli* compared to *A. baumannii*. A. baumanni produces a hepta-acylated lipid A compared to the hexa-
467 acylated lipid A of E. coli, which increases the hydrophobicity in the membrane. In addition, it can survive
468 in absence of lipooligosaccharide and Lipid A, the latest known to be essential for cell survival.[60]

469 Vancomycin is a large hydrophilic molecule, which is usually not effectively sensitized by cationic agents
470 that increase the outer membrane permeability like pentamidine, for example. These agents alter the LPS
471 outer leaflet facilitating the diffusion of drugs across the outer membrane, but they do not damage the
472 integrity of the outer membrane causing membrane disruption. These changes are not enough to facilitate
473 the uptake of large hydrophilic molecules like Vancomycin.[61, 11, 62] Unlike PAs, cationic agents such as

474 pentamidine do not present an hydrophobic moiety on their structures affecting the ability of these
475 molecules to deeply permeate the lipid membrane. The "derivatization-for-sensitization approach" is
476 described in the literature as a successful strategy to sensitize vancomycin and increase drug uptake.[62] In
477 this approach, a combination of a vancomycin-derivative containing a lipo-cationic moiety and a symmetric
478 di-cationic small molecule leads to membrane disruption by cooperative membrane binding and promotes
479 the uptake of vancomycin. It is worth mentioning that only a few of vancomycin's drug adjuvants described
480 in the literature present cationic and hydrophobic characteristics.[62] Those molecules are similar to our PAs
481 (cationic and hydrophobic), which may work as new molecules with the ability to sensitize gram-negative
482 pathogens against vancomycin. Together, these findings indicate that the ability of the PAs to sensitize
483 antibiotic drugs is probably strongly related to their ability to change membrane permeability.

484

485 **3.4. PAs affect the inner-membrane permeability of _E. coli_.**

486

487 To have some insights on the mechanism of action of PA1 + vancomycin drug combination, PA2, and PA3,
488 we studied inner membrane (IM) permeability using a Propidium Iodide uptake assay. The fluorescence
489 intensity of PI in cells treated with PAs and the drug combination are shown in figure 3A. Polymyxin B
490 was used as a positive control to indicate increased inner-membrane permeability. The results show that
491 PA1 at 4 µg/mL (1/8 of the MIC) have shown a relatively smaller PI fluorescence compared to other
492 treatments indicating low permeability of the IM, however the cells treated with PA1 at $1 \times$ MIC (32
493 µg/mL) and $2 \times$ MIC (64 µg/mL) have shown considerably higher PI fluorescence when compared to the
494 positive control polymyxin B indicating greater IM permeability. The drug combination (PA1 +
495 vancomycin) at concentrations of 4 µg/mL:4µg/mL (FICi) showed an increased PI fluorescence compared
496 to the untreated control and the combination at $2 \times$ FICi exhibit greater PI fluorescence compared to the
497 positive control polymyxin B. As expected, vancomycin alone did not induce membrane permeability at 4
498 µg/mL (1/32 of the MIC) and at the MIC value of this drug alone (MIC=128 µg/mL). Together these results
499 indicate that PA1 alone increases the IM permeability in a dose-dependent manner, and PA1 in combination
500 with vancomycin presents a synergistic mechanism of action that further increases the inner-membrane
501 permeability of _E. coli_ in consequence of bacteria death, since these drugs alone did not induce IM
502 permeability at the FICi concentrations.

503 Since the PA molecules present both cationic and hydrophobic characteristics, we proposed that 1) PA1 is
504 able to disrupt the inner membrane of _E. coli_ in a dose-dependent manner causing a small permeabilization
505 at sub-MIC concentrations. Also, we hypothesize that at sub-MIC concentrations PA1 is able to fully
506 disrupt the outer membrane of the _E. coli_ with little effect on the inner membrane. 2) The cationic moiety
507 of the PA1 targets the negatively charged lipids in the outer membrane and the lipid tail then permeates the
508 hydrophobic bilayer causing outer membrane damage/ disruption and increasing permeability. 3)
509 As a result, there is a rapid increase in the accumulation of vancomycin in the cells and in combination with
510 the metabolic perturbations lead to greater cell death. 4) Vancomycin is known to bind to the d-Ala-d-Ala
511 terminus of the peptidoglycan (PG) cell wall precursor lipid II and prevent synthesis of cell wall.[63, 64] 5)
512 PA1 and Vancomycin behave differently when used alone but when used in combination these drugs
513 displayed increased inner membrane permeability. These findings suggest a cooperative mechanism of PA1
514 and Vancomycin that increases the inner membrane permeability of these drugs in combination. Figure 4
515 illustrates the proposed mechanism of action of these drugs in combination. A similar mechanism is also
516 proposed for antimicrobial hexadecapeptide used in combination with vancomycin.[65]
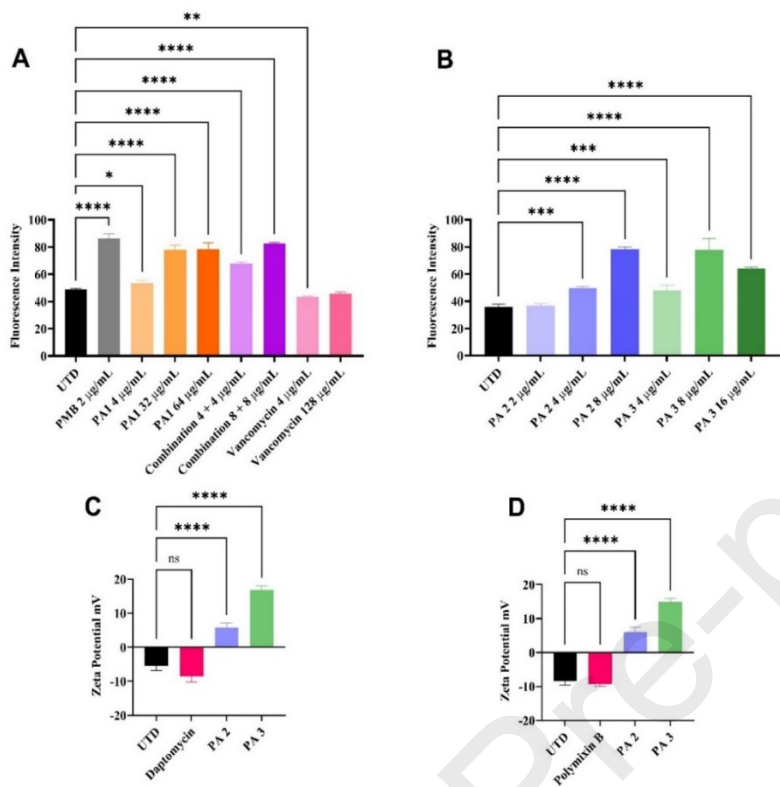
Figure 3: Mechanism of action of PAs on bacteria membrane. A) Propidium iodide uptake of *E. coli* K12 treat with PA1 and PA1 in combination with Vancomycin at different concentrations. B) Propidium iodide uptake of *E. coli* K12 treat with PA2 and PA3. C) Zeta Potential of *S. aureus* MRSA JE2 after treatment with PA2 and PA3 at 40 μg/mL and 80 μg/mL, respectively. D) Zeta Potential of *E. coli* K12 after treatment with at 40 μg/mL and 80 μg/mL, respectively. *Represents $p < 0.05$.

517

518

519 Figure 3B shows the PI uptake assay of *E. coli* cells treated with PA2 and PA3 at different concentrations.
520 The PA2 at 4 μg/mL (1/2 MIC) did not show significant PI fluorescence, PA2 at 8 μg/mL (MIC) and 16
521 μg/mL (2 × MIC) presented an increased PI florescence indicating inner membrane permeability. Similar
522 results were observed when *E. coli* was treated with PA3. Both PA2 and PA3 indicate inner membrane
523 permeability in a dose-dependent manner.

524 The Zeta potential studies have been reported as an important tool to study the interaction of cationic
525 compounds with bacteria membranes surface because these interactions are mostly governed by
526 electrostatic interactions between the positively charge PAs and negatively charged bacteria membrane in
527 addition to hydrophobic interactions.[66, 67] We studied the changes in the bacteria membrane potential of
528 MRSA E. coli after treatment with PA2 and PA3 and the results are presented in figure 3C and 3D.
529 Daptomycin and Polymyxin B were used as standard drugs for MRSA and *E. coli* respectively.
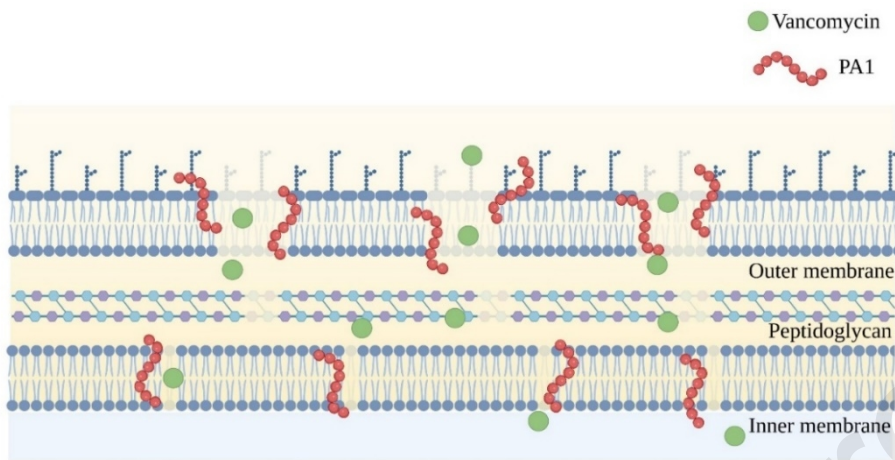
Figure 4: Proposed mechanism for synergistic antibacterial activity of the drug combination (PA1 + Vancomycin) in *E. coli.*

530

531 Zeta potential of untreated MRSA and E coli were found to be – 5.52 mV for MRSA and -8.44 mV for *E.*
532 *coli*. The higher negative electric potential of untreated *E.coli* cells compared to MRSA is attributed to the
533 additional layer of negatively charged LPS present in gram-negative bacteria, these results are similar to
534 other reports in the literature.[66, 68] Daptomycin and Polymyxin B did not significantly change the membrane
535 potential of MRSA and *E.coli* at 20 μg/mL, which is correspondent to 10 × MIC for the drugs. These can
536 be explained by the lower concentrations used in our assays. According to the previous report, Polymyxin
537 B failed to change the membrane potential of MRSA and the changes observed in *E. coli* were dose
538 dependent showing about 10% of zeta potential change at lower concentrations as used in our assay.[66]
539 Daptomycin has an anionic characteristic, it binds to CA^{2+} ions in present in the membrane, which gives it
540 amphiphilic character similar to AMPs[69], these mechanism could explain why Daptomycin does not cause
541 changes in the membrane potential.

542 However, PA2 and PA3 have shown a significant shift in the zeta potential with positive values for both
543 MRSA (figure 3C) and *E.coli* (figure 3D) after 1 hour treatment at 40 μg/mL of PA2 and 80 μg/mL of PA3
544 (10 × MIC) compared to the untreated control. These findings show that PA2 and PA3 neutralized the
545 membrane surface charge, destabilizing the membrane and increasing the permeability. The surface charge
546 neutralization has directly linked to increased membrane permeability in previous studies.[70] These
547 findings are supported by the PI uptake assays showing increase of membrane permeability of E. coli cells
548 at even lower concentrations of 1 × MIC.

549 We further investigated the effect of PAs on bacteria cells morphology by SEM (Figure 5). *S. aureus* and
550 *E. coli* showed substantial morphology changes on membrane surface presenting severe membrane
551 deformations with protruding bumps, holes, and cytoplasmatic leakage after treatment with PA2. Untreated
552 *S. aureus* and *E. coli* showed a smooth and normal membrane surface as seen in Figure 5. Together these
553 results indicate that the mechanism of action of PAs is associated with membrane damage, which is
554 supported by other reports in the literature.[27, 71]
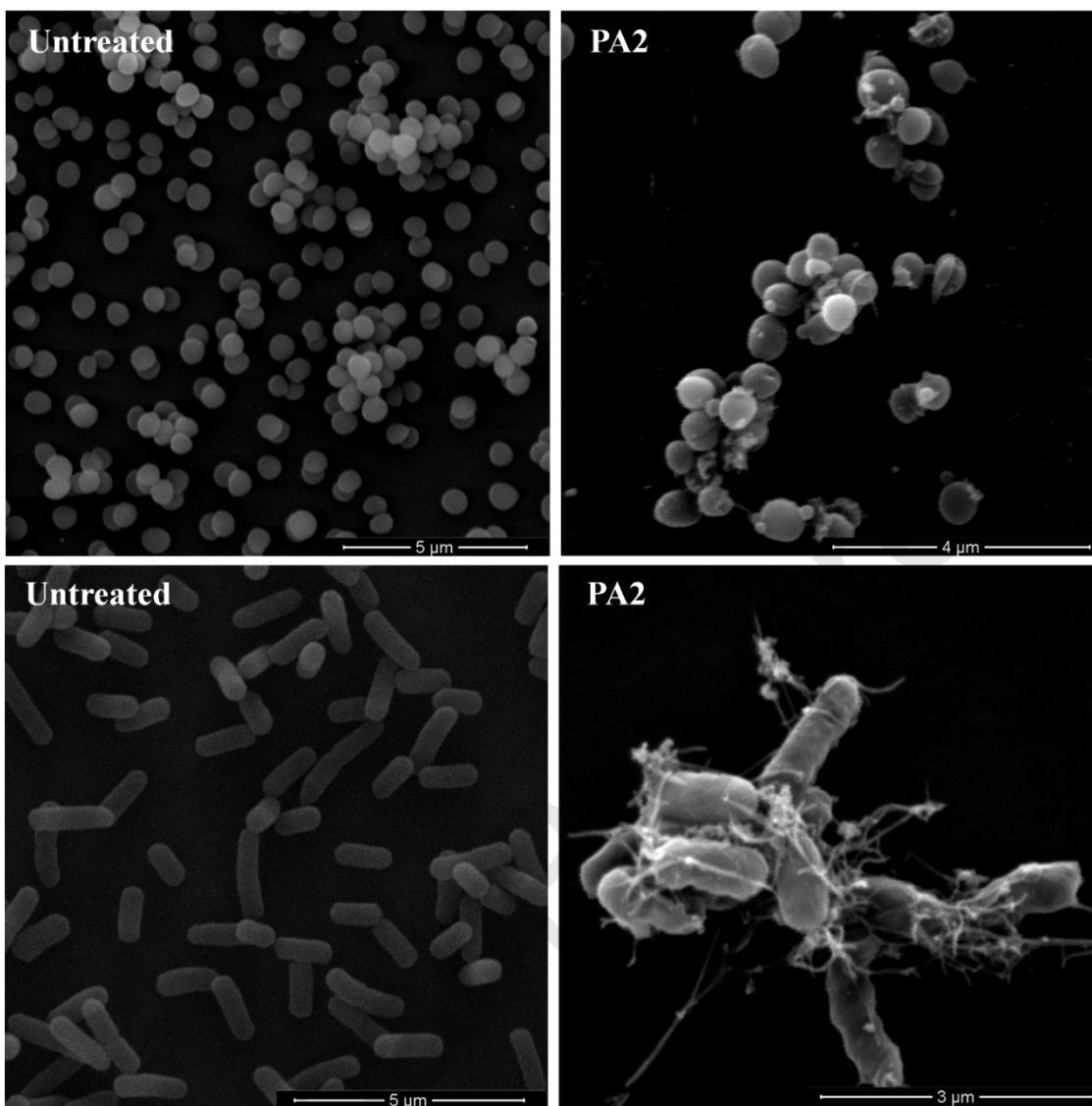
Figure 5: SEM micrographs of *S. aureus* (top) and *E. coli* (bottom) after treatment with PA2 at 8 μg/mL (2X MIC). Untreated bacteria (with no PA addition) were used as a control.

555

3.5. PAs show a low rate of resistance over a period of 21 days.

557 We studied the resistance generation rate for selective PAs against MRSA JE*2* (Figure 6A) and *E. coli*
558 K12 (Figure 6B) using the microdilution in broth method over a period of 21 days. As shown in Figure
559 6A, the MIC of PA2 against *S. aureus* did not change over 21 days indicating that PA2 was not
560 susceptible to drug resistance while PA3 exhibit a two-fold increase of MIC after day 5. Vancomycin also
561 exhibits a two-fold increase of MIC after 19 days. The low rate of resistance for PA3 and the lack of
562 resistance displayed by PA2 is likely due to their mechanism of action associated with membrane
563 disruption. In contrast PA1 alone and PA1 in combination with vancomycin displayed an 8-fold increase
564 of MIC over a period of 21 days with slower development of resistance for PA1 alone. Gentamycin did
565 not show significant susceptibility to drug resistance during the tested period. We believe that PA1 alters
566 the membrane permeability but does not disrupt the membrane facilitating the development of resistance
567 over time. The mechanism of resistance in PA1 could be mediated by changes in the membrane surface

568 by increasing the positive charge, which leads to electrostatic repulsion, similar to the mechanism of
569 daptomycin resistance.[72]
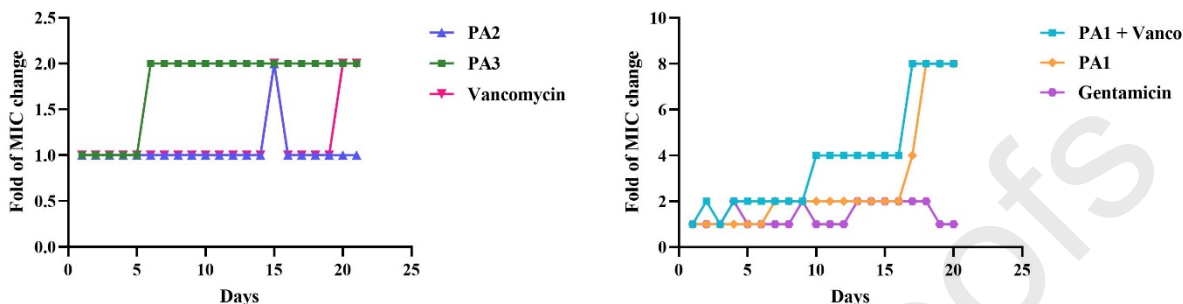
Figure 6: Resistance generation studies. A) Resistance generation for PA2, PA3 and Vancomycin against *S. aureus* MRSA JE2 over 21 days. B) Resistance generation studies for PA1, PA1 in combination with Vancomycin (1:1 ratio) and Gentamicin against *E. coli* K12 over 21 days.

570

3.6. Cytotoxicity

572 We evaluated the toxicity of selected PAs against HEK-293 using the XTT assay and the cell viability is
573 shown in figure 7A. PA2 and PA3 did not present toxicity against the cell line tested up to 8-16 × MIC
574 values. PA1 also did not present toxicity to the cells up to 16 × MIC of PA1 compared to the concentration
575 of antimicrobial activity in combination with vancomycin (MIC=4 µg/mL). Overall, the cells exhibit about
576 100% of viability up to a concentration of 64µg/mL, which is much lower compared to their MIC values
577 against all bacteria strains tested. These results show the great potential of the PAs as antibacterial drugs
578 encouraging us to further study the mechanism of action and the efficacy of these PAs in *in vivo* models in
579 the future.

580 We also studied the hemolytic activity (Supporting Information SI8) of the PAs against red blood cells and
581 the % of hemolyzed cells at 8 µg/mL are shown in the figure 5B. PA1 shows 28.2 % of cell lysis at 8 µg/mL,
582 and this concentration corresponds to 2 × *FICi* of the PA1 in combination with Vancomycin. We expect
583 that PA1 will have a lower hemolytic activity at the *FICi* concentration, but still more studies are needed
584 in order to develop more selective PAs. PA3 and PA4 show 33.3% and 30.6 % of cell lysis at 8 µg/mL,
585 respectively. We observed some correlations between the hemolytic activity, hydrophobicity, and charge
586 among the designed PAs. The most hemolytic PA9 at the concentration tested showed lower zeta potential
587 values and higher hydrophobicity compared to the less hemolytic PA8. Both PA 2 and PA3 (the best
588 antibacterial PAs) were less hydrophobic than PA8, which is shifted toward less hydrophobicity, however
589 both PA2 and PA3 presented a lower positive zeta potential compared to PA8. Hemolytic activity has been
590 linked to higher hydrophobicity which is an important characteristic of membrane active peptides. More
591 studies of structure-toxicity relationship and the development of new strategies such the use of D- amino
592 acids for example are necessary to improve the therapeutical window of these PAs.[73] In addition, the use
593 and development of other potential drug combination therapies with synergistic mechanism of action
594 similar to what we found with PA1 and Vancomycin may lead to new approaches that requires lower
595 concentrations of drugs to achieve antibacterial activity. The use of lower concentrations as an approach is
596 another strategy to overcome the potential toxicity of these PAs."
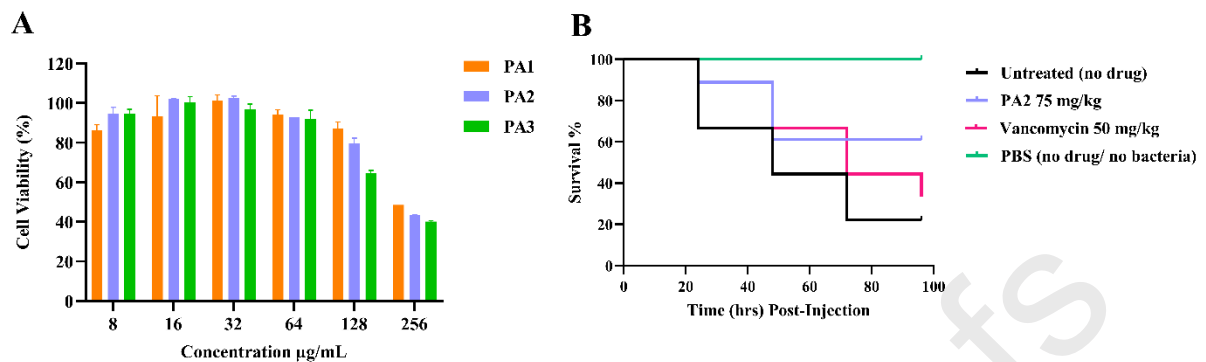
Figure 7: Toxicity of selected PAs. A) Cytotoxicity of selected PAs against HEK-293 cells using XTT assay. B) Antibacterial *in vivo* assay against MRSA JE2 infection in *G. mellonella* model.

597

598 Due to the pH response activity of the Dap rich peptides and the similarities in charge of bacteria cell
599 membrane and cancer cells, the viability of HT-29 cells following treatment with PA6, PA7, PA8 and PA9
600 was determined in both physiological (pH 7.4) and acidic (pH 6.5) conditions using the MTT assay. The
601 cancer cell membranes are negatively charged with extracellular pH of 6.2-6.9 which is similar to the
602 negatively surface charge of bacteria membrane, this characteristics of cancer cell membranes is due to the
603 presence of negatively charged lipids such as phosphatidylserine and phosphatidylethanolamine in the outer
604 leaflet compared to normal cell membrane where these lipids are present in the inner leaflet.[74] Increases in
605 the IC_{50} values for the physiological conditions compared to the acidic conditions were observed for every
606 PA with an IC_{50} that was measurable within the tested concentrations. PA 6 had IC_{50} values of 61.8 μg/mL
607 at pH 6.5 and 71.7 μg/mL at pH 7.4. PA 8 had IC_{50} values of 72.3 μg/mL at pH 6.5 and 126.4 μg/mL at pH
608 7.4. PA 9 had IC_{50} values of 81.7 μg/mL at pH 6.5 and 117.3 μg/mL at pH 7.4. These results indicate a
609 decrease in cytotoxicity in physiological conditions (pH=7.5) for PA6, PA8, and PA9. PA 7 showed no
610 measurable IC_{50} value at both pH conditions, indicating low cytotoxicity at the tested concentrations. Cells
611 in acidic conditions treated with 125 μg/mL of PA8 neared complete loss of viability, and at 250 μg/mL,
612 no viable cells remained. However, when cells in physiological conditions were treated with PA8, viable
613 cells remained even at the highest treatment concentration, 500 μg/mL (Supporting Information, Figure
614 SI9), suggesting that the cytotoxicity might be related to charged residues. Even though these peptides
615 presented a relatively higher hydrophobicity, the lower toxicity of these peptides at pH 7 could be attributed
616 to the amino groups of the side chain being nearly deprotonated and neutral. The PA6, PA7 and PA8 present
617 a net charge of 0 at pH 7 and PA10 present a +2 charge at pH7. The positively charged residues in PA6 are
618 near to the side chain and not at the surface of the micelle, possibly explaining the lower toxicity.

619 **3.7. *In vivo* antibacterial assays in *Galleria mellonella*: PA2 shows potent anti MRSA activity and low
620 toxicity.**

621 We assessed the *in vivo* antibacterial activity of PA2 against MRSA JE2 using *G. mellonella* animal model
622 and the results are presented in figure 7B. PA2 was selected for these studies due to its great antibacterial
623 activity and low rate of resistance. First, we determined the *in vivo* toxicity of PA2 at different
624 concentrations. Animals treated with PA2 at 75 mg/kg body weight have shown 100% survival after 4 days
625 and animals treated with PA2 at 125 and 150 mg/kg body weight have shown 80% survival after 4 days
626 indicating low *in vivo* toxicity of this peptide. These results are included in the supporting information SI10.
627 After determining the safe doses of PA2, we evaluated the antibacterial in vivo activity of PA2 in animals

infected with MRSA. PA2 displayed great antibacterial *in vivo* activity with 60% survival after 4 days with a single dose treatment of PA2 at 75 mg/kg body weight. Vancomycin displayed about 30% of survival after 4 days. These results indicate that PA2 is more effective than vancomycin to treat MRSA infections in this animal model.

4. Conclusion

In this work, we designed a small library of PAs and evaluated their antibacterial activity against gram-positive and gram-negative strains. Our findings indicate that the cationic charges, hydrophobicity morphology and stability of the self-assembled nanostructures play an important role in the antibacterial activity of these compounds. The toxicity of these compounds in red blood cells has been shown to be related with hydrophobicity and charge and it seems to be a very short window of hydrophobicity and charge balance that leads to low toxicity. PA1 demonstrated a very low antibacterial activity alone but it was able to potentiate the activity of Vancomycin with E. coli by a cooperative mechanism that leads to increased inner membrane permeability. This drug combination approach is a very promising approach to overcome the toxicity of PAs since sub-MIC concentrations are required for activity. In addition, PA2 and PA3 have shown potent broad-spectrum antibacterial activity against the strains tested. PA2 was the best candidate in this study showing low development of bacterial resistance and great *in vivo* activity. These findings are promising and open opportunities to further study the mechanism of action of drug combinations and the development of novel antibacterial PAs to overcome bacteria resistance.

5. Acknowledge and Funding

Reference

(1)   CDC. COVID-19: U.S. Impact on Antimicrobial Resistance, Special Report 2022. Atlanta, GA: U.S. Department of Health and Human Services, CDC; 2022.

(2)   CDC. Antibiotic Resistance Threats in the United States, 2019. Atlanta, GA: U.S. Department of Health and Human Services, CDC; 2019.

(3)   2019 Antibacterial Agents in Clinical Development: An Analysis of the Antibacterial Clinical Development Pipeline. Geneva: World Health Organization; 2019. Licence: CC BY-NC-SA 3.0 IGO.

(4)   2021 Antibacterial Agents in Clinical and Preclinical Development: An Overview and Analysis. Geneva: World Health Organization; 2022. Licence: CC BY-NC-SA 3.0 IGO.

666 (5) Breijyeh, Z.; Jubeh, B.; Karaman, R. Resistance of Gram-Negative Bacteria to Current
667 Antibacterial Agents and Approaches to Resolve It. *Molecules* **2020**, *25* (6).
668 https://doi.org/10.3390/molecules25061340.

669 (6) Delcour, A. H. Outer Membrane Permeability and Antibiotic Resistance. *Biochimica et*
670 *Biophysica Acta (BBA) - Proteins and Proteomics* **2009**, *1794* (5), 808–816.
671 https://doi.org/10.1016/j.bbapap.2008.11.005.

672 (7) MacNair Craig R.; Brown Eric D. Outer Membrane Disruption Overcomes Intrinsic, Acquired,
673 and Spontaneous Antibiotic Resistance. *mBio* **2020**, *11* (5), e01615-20.
674 https://doi.org/10.1128/mBio.01615-20.

675 (8) Mielke M, Oltmanns P, Ross B, Rotter M, Schmithausen RM, Sonntag HG, Trautmann M.
676 Antibiotic Resistance: What Is so Special about Multidrug-Resistant Gram-Negative Bacteria? GMS Hyg
677 Infect Control. 2017 Apr 10;12:Doc05. Doi: 10.3205/Dgkh000290. PMID: 28451516; PMCID:
678 PMC5388835.

679 (9) Zeng D, Debabov D, Hartsell TL, Cano RJ, Adams S, Schuyler JA, McMillan R, Pace JL.
680 Approved Glycopeptide Antibacterial Drugs: Mechanism of Action and Resistance. Cold Spring Harb
681 Perspect Med. 2016 Dec 1;6(12):A026989. Doi: 10.1101/Cshperspect.A026989. PMID: 27663982;
682 PMCID: PMC5131748.

683 (10) Stokes, J. M.; MacNair, C. R.; Ilyas, B.; French, S.; Côté, J.-P.; Bouwman, C.; Farha, M. A.;
684 Sieron, A. O.; Whitfield, C.; Coombes, B. K.; Brown, E. D. Pentamidine Sensitizes Gram-Negative
685 Pathogens to Antibiotics and Overcomes Acquired Colistin Resistance. *Nature Microbiology* **2017**, *2* (5),
686 17028. https://doi.org/10.1038/nmicrobiol.2017.28.

687 (11) Zhou, Y.; Huang, W.; Lei, E.; Yang, A.; Li, Y.; Wen, K.; Wang, M.; Li, L.; Chen, Z.; Zhou, C.;
688 Bai, S.; Han, J.; Song, W.; Ren, X.; Zeng, X.; Pu, H.; Wan, M.; Feng, X. Cooperative Membrane Damage
689 as a Mechanism for Pentamidine–Antibiotic Mutual Sensitization. *ACS Chem. Biol.* **2022**, *17* (11), 3178–
690 3190. https://doi.org/10.1021/acschembio.2c00613.

691 (12) Sands, M.; Kron, M. A.; Brown, R. B. Pentamidine: A Review. *Reviews of Infectious Diseases*
692 **1985**, *7* (5), 625–6344. https://doi.org/10.1093/clinids/7.5.625.

693 (13) Kuryshev, Y. A.; Ficker, E.; Wang, L.; Hawryluk, P.; Dennis, A. T.; Wible, B. A.; Brown, A. M.;
694 Kang, J.; Chen, X.-L.; Sawamura, K.; Reynolds, W.; Rampe, D. Pentamidine-Induced Long QT
695 Syndrome and Block of hERG Trafficking. *J Pharmacol Exp Ther* **2005**, *312* (1), 316.
696 https://doi.org/10.1124/jpet.104.073692.

697 (14) Mohammed, E. H. M.; Lohan, S.; Ghaffari, T.; Gupta, S.; Tiwari, R. K.; Parang, K. Membrane-
698 Active Cyclic Amphiphilic Peptides: Broad-Spectrum Antibacterial Activity Alone and in Combination
699 with Antibiotics. *J. Med. Chem.* **2022**, *65* (23), 15819–15839.
700 https://doi.org/10.1021/acs.jmedchem.2c01469.

701 (15) Zeng, P.; Xu, C.; Liu, C.; Liu, J.; Cheng, Q.; Gao, W.; Yang, X.; Chen, S.; Chan, K.-F.; Wong,
702 K.-Y. De Novo Designed Hexadecapeptides Synergize Glycopeptide Antibiotics Vancomycin and
703 Teicoplanin against Pathogenic Klebsiella Pneumoniae via Disruption of Cell Permeability and Potential.
704 *ACS Appl. Bio Mater.* **2020**, *3* (3), 1738–1752. https://doi.org/10.1021/acsabm.0c00044.

705 (16) Mood, E. H.; Goltermann, L.; Brolin, C.; Cavaco, L. M.; Nejad, A. J.; Yavari, N.; Frederiksen,
706 N.; Franzyk, H.; Nielsen, P. E. Antibiotic Potentiation in Multidrug-Resistant Gram-Negative Pathogenic

Bacteria by a Synthetic Peptidomimetic. *ACS Infect. Dis.* **2021**, *7* (8), 2152–2163. https://doi.org/10.1021/acsinfecdis.1c00147.

(17)   Kang, H. K.; Park, J.; Seo, C. H.; Park, Y. PEP27-2, a Potent Antimicrobial Cell-Penetrating Peptide, Reduces Skin Abscess Formation during Staphylococcus Aureus Infections in Mouse When Used in Combination with Antibiotics. *ACS Infect. Dis.* **2021**, *7* (9), 2620–2636. https://doi.org/10.1021/acsinfecdis.0c00894.

(18)   Konai, M. M.; Haldar, J. Lysine-Based Small Molecule Sensitizes Rifampicin and Tetracycline against Multidrug-Resistant Acinetobacter Baumannii and Pseudomonas Aeruginosa. *ACS Infect. Dis.* **2020**, *6* (1), 91–99. https://doi.org/10.1021/acsinfecdis.9b00221.

(19)   Shao, Z.; Wulandari, E.; Lin, R. C. Y.; Xu, J.; Liang, K.; Wong, E. H. H. Two plus One: Combination Therapy Tri-Systems Involving Two Membrane-Disrupting Antimicrobial Macromolecules and Antibiotics. *ACS Infect. Dis.* **2022**, *8* (8), 1480–1490. https://doi.org/10.1021/acsinfecdis.2c00087.

(20)   Namivandi-Zangeneh, R.; Sadrearhami, Z.; Dutta, D.; Willcox, M.; Wong, E. H. H.; Boyer, C. Synergy between Synthetic Antimicrobial Polymer and Antibiotics: A Promising Platform To Combat Multidrug-Resistant Bacteria. *ACS Infect. Dis.* **2019**, *5* (8), 1357–1365. https://doi.org/10.1021/acsinfecdis.9b00049.

(21)   Mahlapuu, M.; Håkansson, J.; Ringstad, L.; Björn, C. Antimicrobial Peptides: An Emerging Category of Therapeutic Agents. *Frontiers in Cellular and Infection Microbiology* **2016**, *6*.

(22)   Ding, Y.; Ting, J. P.; Liu, J.; Al-Azzam, S.; Pandya, P.; Afshar, S. Impact of Non-Proteinogenic Amino Acids in the Discovery and Development of Peptide Therapeutics. *Amino Acids* **2020**, *52* (9), 1207–1226. https://doi.org/10.1007/s00726-020-02890-9.

(23)   Hamley, I. W. Lipopeptides: From Self-Assembly to Bioactivity. *Chem. Commun.* **2015**, *51* (41), 8574–8583. https://doi.org/10.1039/C5CC01535A.

(24)   Zhang, Q.-Y.; Yan, Z.-B.; Meng, Y.-M.; Hong, X.-Y.; Shao, G.; Ma, J.-J.; Cheng, X.-R.; Liu, J.; Kang, J.; Fu, C.-Y. Antimicrobial Peptides: Mechanism of Action, Activity and Clinical Potential. *Military Medical Research* **2021**, *8* (1), 48. https://doi.org/10.1186/s40779-021-00343-2.

(25)   Huan, Y.; Kong, Q.; Mou, H.; Yi, H. Antimicrobial Peptides: Classification, Design, Application and Research Progress in Multiple Fields. *Frontiers in Microbiology* **2020**, *11*.

(26)   Rosenfeld, Y.; Lev, N.; Shai, Y. Effect of the Hydrophobicity to Net Positive Charge Ratio on Antibacterial and Anti-Endotoxin Activities of Structurally Similar Antimicrobial Peptides. *Biochemistry* **2010**, *49* (5), 853–861. https://doi.org/10.1021/bi900724x.

(27)   Rodrigues de Almeida, N.; Han, Y.; Perez, J.; Kirkpatrick, S.; Wang, Y.; Sheridan, M. C. Design, Synthesis, and Nanostructure-Dependent Antibacterial Activity of Cationic Peptide Amphiphiles. *ACS Appl. Mater. Interfaces* **2019**, *11* (3), 2790–2801. https://doi.org/10.1021/acsami.8b17808.

(28)   Conda-Sheridan, M.; Lee, S. S.; Preslar, A. T.; Stupp, S. I. Esterase-Activated Release of Naproxen from Supramolecular Nanofibres. *Chem. Commun.* **2014**, *50* (89), 13757–13760. https://doi.org/10.1039/C4CC06340F.

744 (29)   Zaldivar, G.; Vemulapalli, S.; Udumula, V.; Conda-Sheridan, M.; Tagliazucchi, M. Self-
745 Assembled Nanostructures of Peptide Amphiphiles: Charge Regulation by Size Regulation. *J. Phys.*
746 *Chem. C* **2019**, *123* (28), 17606–17615. https://doi.org/10.1021/acs.jpcc.9b04280.

747 (30)   Ye, M.; Zhao, Y.; Wang, Y.; Zhao, M.; Yodsanit, N.; Xie, R.; Andes, D.; Gong, S. A Dual-
748 Responsive Antibiotic-Loaded Nanoparticle Specifically Binds Pathogens and Overcomes Antimicrobial-
749 Resistant Infections. *Advanced Materials* **2021**, *33* (9), 2006772.
750 https://doi.org/10.1002/adma.202006772.

751 (31)   Blaskovich, M. A. T.; Kavanagh, A. M.; Elliott, A. G.; Zhang, B.; Ramu, S.; Amado, M.; Lowe,
752 G. J.; Hinton, A. O.; Pham, D. M. T.; Zuegg, J.; Beare, N.; Quach, D.; Sharp, M. D.; Pogliano, J.; Rogers,
753 A. P.; Lyras, D.; Tan, L.; West, N. P.; Crawford, D. W.; Peterson, M. L.; Callahan, M.; Thurn, M. The
754 Antimicrobial Potential of Cannabidiol. *Communications Biology* **2021**, *4* (1), 7.
755 https://doi.org/10.1038/s42003-020-01530-y.

756 (32)   Ma, Z.; Kim, D.; Adesogan, A. T.; Ko, S.; Galvao, K.; Jeong, K. C. Chitosan Microparticles
757 Exert Broad-Spectrum Antimicrobial Activity against Antibiotic-Resistant Micro-Organisms without
758 Increasing Resistance. *ACS Appl. Mater. Interfaces* **2016**, *8* (17), 10700–10709.
759 https://doi.org/10.1021/acsami.6b00894.

760 (33)   Ignasiak, K.; Maxwell, A. Galleria Mellonella (Greater Wax Moth) Larvae as a Model for
761 Antibiotic Susceptibility Testing and Acute Toxicity Trials. *BMC Research Notes* **2017**, *10* (1), 428.
762 https://doi.org/10.1186/s13104-017-2757-8.

763 (34)   Li, L.; Vorobyov, I.; Allen, T. W. The Different Interactions of Lysine and Arginine Side Chains
764 with Lipid Membranes. *J. Phys. Chem. B* **2013**, *117* (40), 11906–11920.
765 https://doi.org/10.1021/jp405418y.

766 (35)   Dong, N.; Wang, C.; Zhang, T.; Zhang, L.; Xue, C.; Feng, X.; Bi, C.; Shan, A. Bioactivity and
767 Bactericidal Mechanism of Histidine-Rich β-Hairpin Peptide Against Gram-Negative Bacteria.
768 *International Journal of Molecular Sciences* **2019**, *20* (16). https://doi.org/10.3390/ijms20163954.

769 (36)   Bi, X.; Wang, C.; Dong, W.; Zhu, W.; Shang, D. Antimicrobial Properties and Interaction of Two
770 Trp-Substituted Cationic Antimicrobial Peptides with a Lipid Bilayer. *The Journal of Antibiotics* **2014**, *67*
771 (5), 361–368. https://doi.org/10.1038/ja.2014.4.

772 (37)   Isom, D. G.; Castañeda, C. A.; Cannon, B. R.; García-Moreno E., B. Large Shifts in pKa Values
773 of Lysine Residues Buried inside a Protein. *Proceedings of the National Academy of Sciences* **2011**, *108*
774 (13), 5260–5265. https://doi.org/10.1073/pnas.1010750108.

775 (38)   Cote, Y.; Fu, I. W.; Dobson, E. T.; Goldberger, J. E.; Nguyen, H. D.; Shen, J. K. Mechanism of
776 the pH-Controlled Self-Assembly of Nanofibers from Peptide Amphiphiles. *J. Phys. Chem. C* **2014**, *118*
777 (29), 16272–16278. https://doi.org/10.1021/jp5048024.

778 (39)   Cui, H.; Webber, M. J.; Stupp, S. I. Self-Assembly of Peptide Amphiphiles: From Molecules to
779 Nanostructures to Biomaterials. *Peptide Science* **2010**, *94* (1), 1–18. https://doi.org/10.1002/bip.21328.

780 (40)   Hendricks, M. P.; Sato, K.; Palmer, L. C.; Stupp, S. I. Supramolecular Assembly of Peptide
781 Amphiphiles. *Acc. Chem. Res.* **2017**, *50* (10), 2440–2448. https://doi.org/10.1021/acs.accounts.7b00297.

(41)   Paramonov, S. E.; Jun, H.-W.; Hartgerink, J. D. Self-Assembly of Peptide−Amphiphile Nanofibers: The Roles of Hydrogen Bonding and Amphiphilic Packing. *J. Am. Chem. Soc.* **2006**, *128* (22), 7291–7298. https://doi.org/10.1021/ja060573x.

(42)   Boothroyd, S.; Saiani, A.; Miller, A. F. Controlling Network Topology and Mechanical Properties of Co-Assembling Peptide Hydrogels. *Biopolymers* **2014**, *101* (6), 669–680. https://doi.org/10.1002/bip.22435.

(43)   Chen, Y.; Gan, H. X.; Tong, Y. W. pH-Controlled Hierarchical Self-Assembly of Peptide Amphiphile. *Macromolecules* **2015**, *48* (8), 2647–2653. https://doi.org/10.1021/ma502572w.

(44)   Li, L.; Vorobyov, I.; Allen, T. W. The Different Interactions of Lysine and Arginine Side Chains with Lipid Membranes. *J. Phys. Chem. B* **2013**, *117* (40), 11906–11920. https://doi.org/10.1021/jp405418y.

(45)   Selvamani, V. Chapter 15 - Stability Studies on Nanomaterials Used in Drugs. In *Characterization and Biology of Nanomaterials for Drug Delivery*; Mohapatra, S. S., Ranjan, S., Dasgupta, N., Mishra, R. K., Thomas, S., Eds.; Elsevier, 2019; pp 425–444. https://doi.org/10.1016/B978-0-12-814031-4.00015-5.

(46)   Yang, L.; Chen, C.; Liang, T.; Hao, L.; Gu, Q.; Xu, H.; Zhao, Y.; Jiang, L.; Fan, X. Disassembling Ability of Lipopeptide Promotes the Antibacterial Activity. *Journal of Colloid and Interface Science* **2023**. https://doi.org/10.1016/j.jcis.2023.05.168.

(47)   Chaudhury, S.; Ripoll, D. R.; Wallqvist, A. Structure-Based pKa Prediction Provides a Thermodynamic Basis for the Role of Histidines in pH-Induced Conformational Transitions in Dengue Virus. *Biochemistry and Biophysics Reports* **2015**, *4*, 375–385. https://doi.org/10.1016/j.bbrep.2015.10.014.

(48)   Kacprzyk, L.; Rydengård, V.; Mörgelin, M.; Davoudi, M.; Pasupuleti, M.; Malmsten, M.; Schmidtchen, A. Antimicrobial Activity of Histidine-Rich Peptides Is Dependent on Acidic Conditions. *Biochimica et Biophysica Acta (BBA) - Biomembranes* **2007**, *1768* (11), 2667–2680. https://doi.org/10.1016/j.bbamem.2007.06.020.

(49)   Lan, Y.; Langlet-Bertin, B.; Abbate, V.; Vermeer, L. S.; Kong, X.; Sullivan, K. E.; Leborgne, C.; Scherman, D.; Hider, R. C.; Drake, A. F.; Bansal, S. S.; Kichler, A.; Mason, A. J. Incorporation of 2,3-Diaminopropionic Acid into Linear Cationic Amphipathic Peptides Produces pH-Sensitive Vectors. *ChemBioChem* **2010**, *11* (9), 1266–1272. https://doi.org/10.1002/cbic.201000073.

(50)   Mason A. James; Gasnier Claire; Kichler Antoine; Prévost Gilles; Aunis Dominique; Metz-Boutigue Marie-Hélène; Bechinger Burkhard. Enhanced Membrane Disruption and Antibiotic Action against Pathogenic Bacteria by Designed Histidine-Rich Peptides at Acidic pH. *Antimicrobial Agents and Chemotherapy* **2006**, *50* (10), 3305–3311. https://doi.org/10.1128/AAC.00490-06.

(51)   Wang, Z.; Li, Q.; Li, J.; Shang, L.; Li, J.; Chou, S.; Lyu, Y.; Shan, A. pH-Responsive Antimicrobial Peptide with Selective Killing Activity for Bacterial Abscess Therapy. *J. Med. Chem.* **2022**, *65* (7), 5355–5373. https://doi.org/10.1021/acs.jmedchem.1c01485.

(52)   Mant, C. T.; Jiang, Z.; Gera, L.; Davis, T.; Nelson, K. L.; Bevers, S.; Hodges, R. S. De Novo Designed Amphipathic α-Helical Antimicrobial Peptides Incorporating Dab and Dap Residues on the Polar Face To Treat the Gram-Negative Pathogen, Acinetobacter Baumannii. *J. Med. Chem.* **2019**, *62* (7), 3354–3366. https://doi.org/10.1021/acs.jmedchem.8b01785.

823 (53)   Zelezetsky, I.; Pacor, S.; Pag, U.; Papo, N.; Shai, Y.; Sahl, H.-G.; Tossi, A. Controlled Alteration
824 of the Shape and Conformational Stability of α-Helical Cell-Lytic Peptides: Effect on Mode of Action and
825 Cell Specificity. *Biochemical Journal* **2005**, *390* (1), 177–188. https://doi.org/10.1042/BJ20042138.

826 (54)   Uggerhøj, L. E.; Poulsen, T. J.; Munk, J. K.; Fredborg, M.; Sondergaard, T. E.; Frimodt-Moller,
827 N.; Hansen, P. R.; Wimmer, R. Rational Design of Alpha-Helical Antimicrobial Peptides: Do's and
828 Don'ts. *ChemBioChem* **2015**, *16* (2), 242–253. https://doi.org/10.1002/cbic.201402581.

829 (55)   Dong, W.; Mao, X.; Guan, Y.; Kang, Y.; Shang, D. Antimicrobial and Anti-Inflammatory
830 Activities of Three Chensinin-1 Peptides Containing Mutation of Glycine and Histidine Residues.
831 *Scientific Reports* **2017**, *7* (1), 40228. https://doi.org/10.1038/srep40228.

832 (56)   Hartmann, G. R.; Heinrich, P.; Kollenda, M. C.; Skrobranek, B.; Tropschug, M.; Weiß, W.
833 Molecular Mechanism of Action of the Antibiotic Rifampicin. *Angewandte Chemie International Edition*
834 *in English* **1985**, *24* (12), 1009–1014. https://doi.org/10.1002/anie.198510093.

835 (57)   Odds, F. C. Synergy, Antagonism, and What the Chequerboard Puts between Them. *Journal of*
836 *Antimicrobial Chemotherapy* **2003**, *52* (1), 1–1. https://doi.org/10.1093/jac/dkg301.

837 (58)   Schweizer, L.; Ramirez, D.; Schweizer, F. Effects of Lysine N-ζ-Methylation in Ultrashort
838 Tetrabasic Lipopeptides (UTBLPs) on the Potentiation of Rifampicin, Novobiocin, and Niclosamide in
839 Gram-Negative Bacteria. *Antibiotics* **2022**, *11* (3). https://doi.org/10.3390/antibiotics11030335.

840 (59)   Vaara, M.; Vaara, T. Sensitization of Gram-Negative Bacteria to Antibiotics and Complement by
841 a Nontoxic Oligopeptide. *Nature* **1983**, *303* (5917), 526–528. https://doi.org/10.1038/303526a0.

842 (60)   Powers, M. J.; Trent, M. S. Expanding the Paradigm for the Outer Membrane: Acinetobacter
843 Baumannii in the Absence of Endotoxin. *Molecular Microbiology* **2018**, *107* (1), 47–56.
844 https://doi.org/10.1111/mmi.13872.

845 (61)   Vaara M. Agents That Increase the Permeability of the Outer Membrane. *Microbiological*
846 *Reviews* **1992**, *56* (3), 395–411. https://doi.org/10.1128/mr.56.3.395-411.1992.

847 (62)   Lei, E.; Tao, H.; Jiao, S.; Yang, A.; Zhou, Y.; Wang, M.; Wen, K.; Wang, Y.; Chen, Z.; Chen, X.;
848 Song, J.; Zhou, C.; Huang, W.; Xu, L.; Guan, D.; Tan, C.; Liu, H.; Cai, Q.; Zhou, K.; Modica, J.; Huang,
849 S.-Y.; Huang, W.; Feng, X. Potentiation of Vancomycin: Creating Cooperative Membrane Lysis through
850 a "Derivatization-for-Sensitization" Approach. *J. Am. Chem. Soc.* **2022**, *144* (23), 10622–10639.
851 https://doi.org/10.1021/jacs.2c03784.

852 (63)   Münch Daniela; Engels Ina; Müller Anna; Reder-Christ Katrin; Falkenstein-Paul Hildegard;
853 Bierbaum Gabriele; Grein Fabian; Bendas Gerd; Sahl Hans-Georg; Schneider Tanja. Structural Variations
854 of the Cell Wall Precursor Lipid II and Their Influence on Binding and Activity of the Lipoglycopeptide
855 Antibiotic Oritavancin. *Antimicrobial Agents and Chemotherapy* **2015**, *59* (2), 772–781.
856 https://doi.org/10.1128/aac.02663-14.

857 (64)   Wang, F.; Zhou, H.; Olademehin, O. P.; Kim, S. J.; Tao, P. Insights into Key Interactions
858 between Vancomycin and Bacterial Cell Wall Structures. *ACS Omega* **2018**, *3* (1), 37–45.
859 https://doi.org/10.1021/acsomega.7b01483.

860 (65)   Zeng, P.; Xu, C.; Liu, C.; Liu, J.; Cheng, Q.; Gao, W.; Yang, X.; Chen, S.; Chan, K.-F.; Wong,
861 K.-Y. De Novo Designed Hexadecapeptides Synergize Glycopeptide Antibiotics Vancomycin and

Teicoplanin against Pathogenic Klebsiella Pneumoniae via Disruption of Cell Permeability and Potential. *ACS Appl. Bio Mater.* **2020**, *3* (3), 1738–1752. https://doi.org/10.1021/acsabm.0c00044.

(66)   Halder, S.; Yadav, K. K.; Sarkar, R.; Mukherjee, S.; Saha, P.; Haldar, S.; Karmakar, S.; Sen, T. Alteration of Zeta Potential and Membrane Permeability in Bacteria: A Study with Cationic Agents. *SpringerPlus* **2015**, *4* (1), 672. https://doi.org/10.1186/s40064-015-1476-7.

(67)   Ferreyra Maillard, A. P. V.; Espeche, J. C.; Maturana, P.; Cutro, A. C.; Hollmann, A. Zeta Potential beyond Materials Science: Applications to Bacterial Systems and to the Development of Novel Antimicrobials. *Biochimica et Biophysica Acta (BBA) - Biomembranes* **2021**, *1863* (6), 183597. https://doi.org/10.1016/j.bbamem.2021.183597.

(68)   Alves, C. S.; Melo, M. N.; Franquelim, H. G.; Ferre, R.; Planas, M.; Feliu, L.; Bardají, E.; Kowalczyk, W.; Andreu, D.; Santos, N. C.; Fernandes, M. X.; Castanho, M. A. R. B. Escherichia Coli Cell Surface Perturbation and Disruption Induced by Antimicrobial Peptides BP100 and pepR *. *Journal of Biological Chemistry* **2010**, *285* (36), 27536–27544. https://doi.org/10.1074/jbc.M110.130955.

(69)   Grein, F.; Müller, A.; Scherer, K. M.; Liu, X.; Ludwig, K. C.; Klöckner, A.; Strach, M.; Sahl, H.-G.; Kubitscheck, U.; Schneider, T. Ca2+-Daptomycin Targets Cell Wall Biosynthesis by Forming a Tripartite Complex with Undecaprenyl-Coupled Intermediates and Membrane Lipids. *Nature Communications* **2020**, *11* (1), 1455. https://doi.org/10.1038/s41467-020-15257-1.

(70)   Pérez-Peinado, C.; Dias, S. A.; Domingues, M. M.; Benfield, A. H.; Freire, J. M.; Rádis-Baptista, G.; Gaspar, D.; Castanho, M. A. R. B.; Craik, D. J.; Henriques, S. T.; Veiga, A. S.; Andreu, D. Mechanisms of Bacterial Membrane Permeabilization by Crotalicidin (Ctn) and Its Fragment Ctn(15–34), Antimicrobial Peptides from Rattlesnake Venom. *Journal of Biological Chemistry* **2018**, *293* (5), 1536–1549. https://doi.org/10.1074/jbc.RA117.000125.

(71)   Armas, F.; Pacor, S.; Ferrari, E.; Guida, F.; Pertinhez, T. A.; Romani, A. A.; Scocchi, M.; Benincasa, M. Design, Antimicrobial Activity and Mechanism of Action of Arg-Rich Ultra-Short Cationic Lipopeptides. *PLOS ONE* **2019**, *14* (2), e0212447. https://doi.org/10.1371/journal.pone.0212447.

(72)   Heidary, M.; Khosravi, A. D.; Khoshnood, S.; Nasiri, M. J.; Soleimani, S.; Goudarzi, M. Daptomycin. *Journal of Antimicrobial Chemotherapy* **2018**, *73* (1), 1–11. https://doi.org/10.1093/jac/dkx349.

(73)   Greco, I.; Molchanova, N.; Holmedal, E.; Jenssen, H.; Hummel, B. D.; Watts, J. L.; Håkansson, J.; Hansen, P. R.; Svenson, J. Correlation between Hemolytic Activity, Cytotoxicity and Systemic in Vivo Toxicity of Synthetic Antimicrobial Peptides. *Scientific Reports* **2020**, *10* (1), 13206. https://doi.org/10.1038/s41598-020-69995-9.

(74)   Alves, A. C.; Ribeiro, D.; Nunes, C.; Reis, S. Biophysics in Cancer: The Relevance of Drug-Membrane Interaction Studies. *Biochimica et Biophysica Acta (BBA) - Biomembranes* **2016**, *1858* (9), 2231–2244. https://doi.org/10.1016/j.bbamem.2016.06.025.

Declaration of interests

901 ☒ The authors declare that they have no known competing financial interests or personal relationships
902 that could have appeared to influence the work reported in this paper.

903

904 ☐The authors declare the following financial interests/personal relationships which may be considered
905 as potential competing interests:
906

907
908
909

910

911

912

913